



This is a repository copy of *Extrapolating demography with climate, proximity and phylogeny: approach with caution.*

White Rose Research Online URL for this paper:
<http://eprints.whiterose.ac.uk/106767/>

Version: Accepted Version

Article:

Coutts, S.R., Salguero-Gomez, R., Csergo, A.M. et al. (1 more author) (2016)
Extrapolating demography with climate, proximity and phylogeny: approach with caution.
Ecology Letters, 19 (12). pp. 1429-1438. ISSN 1461-0248

<https://doi.org/10.1111/ele.12691>

Reuse

Unless indicated otherwise, fulltext items are protected by copyright with all rights reserved. The copyright exception in section 29 of the Copyright, Designs and Patents Act 1988 allows the making of a single copy solely for the purpose of non-commercial research or private study within the limits of fair dealing. The publisher or other rights-holder may allow further reproduction and re-use of this version - refer to the White Rose Research Online record for this item. Where records identify the publisher as the copyright holder, users can verify any specific terms of use on the publisher's website.

Takedown

If you consider content in White Rose Research Online to be in breach of UK law, please notify us by emailing eprints@whiterose.ac.uk including the URL of the record and the reason for the withdrawal request.



eprints@whiterose.ac.uk
<https://eprints.whiterose.ac.uk/>

Extrapolating demography with climate, proximity and phylogeny: approach with caution

Shaun R. Coutts^{1,2,3}, Roberto Salguero-Gómez^{1,2,3,4}, Anna M. Csergő³,
Yvonne M. Buckley^{1,3}

October 31, 2016

1. School of Biological Sciences. Centre for Biodiversity and Conservation Science. The University of Queensland, St Lucia, QLD 4072, Australia.
2. Department of Animal and Plant Sciences, University of Sheffield, Western Bank, Sheffield, UK.
3. School of Natural Sciences, Zoology, Trinity College Dublin, Dublin 2, Ireland.
4. Evolutionary Demography Laboratory. Max Planck Institute for Demographic Research. Rostock, DE-18057, Germany.

Keywords: COMPADRE Plant Matrix Database, comparative demography, damping ratio, elasticity, matrix population model, phylogenetic analysis, population growth rate (λ), spatially lagged models

Author statement: SRC developed the initial concept, performed the statistical analysis and wrote the first draft of the manuscript. RSG helped develop the initial concept, provided code for deriving demographic metrics and phylogenetic analysis, and provided the matrix selection criteria. YMB helped develop the initial concept and advised on analysis. All authors made substantial contributions to editing the manuscript and further refining ideas and interpretations.

ABSTRACT

Plant population responses are key to understanding the effects of threats such as climate change and invasions. However, we lack demographic data for most species, and the data we have are often geographically aggregated. We determined to what extent existing data can be extrapolated to predict population performance across larger sets of species and spatial areas. We used 550 matrix models, across 210 species, sourced from the COMPADRE Plant Matrix Database, to model how climate, geographic proximity and phylogeny predicted population performance. Models including only geographic proximity and phylogeny explained 5-40% of the variation in four key metrics of population performance. However, there was poor extrapolation between species and extrapolation was limited to geographic scales smaller than those at which landscape scale threats typically occur. Thus, demographic information should only be extrapolated with caution. Capturing demography at scales relevant to landscape level threats will require more geographically extensive sampling.

INTRODUCTION

Global threats to biodiversity such as climate change, invasive species and land conversion for agriculture affect multiple species at regional and global scales (McGeoch *et al.*, 2010; Hartmann *et al.*, 2013). Invasion and extinction are fundamentally demographic processes, regulated by the vital rates of the population (e.g. survival, growth, reproduction). Consequently, we are pressed to understand and predict how demography responds to environmental conditions across multiple taxa worldwide (Sutherland *et al.*, 2013). Historically, developing such a predictive framework has proven difficult. Even describing demographic patterns across species and regions is challenging due to the lack of both detailed demographic data for multiple species at large geographic scales, and high resolution comparative approaches (but see Blomberg & Garland 2002, Buckley *et al.* 2010, Salguero-Gómez *et al.* 2016). Another challenge is that we often do not understand the underlying factors that drive population responses to environmental gradients (Ehrlén & Morris, 2015). Further, determining the response of every population of every species is impractical. Consequently, we frequently generalize important aspects of population ecology, such as life history strategy (Silvertown *et al.*, 1996; Salguero-Gómez *et al.*, 2016) and invasiveness (Ramula *et al.*, 2008), from a handful of well studied species and populations to wider areas and other species.

Even though demographic studies have been carried out on thousands of species, most of those species have only been studied in a few locations. It is common to then assume that those studies adequately capture the demographic performance of a species across an entire region (Burns *et al.*, 2010; Crone *et al.*, 2011; Salguero-Gómez *et al.*, 2016). However, it is currently unknown how close, both geographically and phylogenetically, populations or species must be before demographic performance can be extrapolated among them. Likewise, it remains unknown which aspects of demographic performance (e.g. population growth rate, recovery from perturbations) are most transferable across populations.

Matrix population models (Caswell, 2001) provide an ideal means to test how transferable population performance metrics are across a wide suite of regions, life histories and taxa within the plant kingdom. To date, matrix population models have been developed for over 1,300 plant species (Salguero-

Gómez *et al.*, 2015). Matrix population models are typically constructed from field measurements and summarise life histories ranging from simple to complex in a standard format (Caswell, 2001). This allows the direct comparison of ecologically and biologically meaningful demographic metrics across populations, species and years (Silvertown *et al.*, 1993; Caswell, 2001; Salguero-Gómez & de Kroon, 2010). These metrics include population growth rate (Tuljapurkar & Orzack, 1980; Caswell, 2001), the underlying impacts of demographic processes (i.e. vital rates of survival, growth and reproduction) on population performance (de Kroon *et al.*, 1986; Caswell, 2001), or the ability of populations to recover from perturbations (Stott *et al.*, 2010).

We focused on the generalisability of four demographic metrics across species and populations: the asymptotic population growth rate (λ), its variation over time, elasticities of λ to demographic processes, and damping ratio (ρ). Previous comparative studies have found that populations of the same species tend to have similar values for λ (Doak & Morris, 2010; Villellas *et al.*, 2015), although other work has shown significant differences among populations of the same species (Silvertown *et al.*, 1996). Comparative studies have found that phylogenetic relationships above the species level do not predict λ (Buckley *et al.*, 2010; Burns *et al.*, 2010). Environment has been found to explain some variation in λ (Buckley *et al.*, 2010). However, the effect of any one environmental variable on λ may be reduced as multiple environmental factors can affect λ . In addition, stable populations can be maintained across environmental gradients by increasing some vital rates to offset decreases in others (Doak & Morris, 2010; Villellas *et al.*, 2015). Temporal variation of population growth rates is expected to increase with increasing environmental constraints due to limitations on vital rates (Gerst *et al.*, 2011). Less evidence exists on how geographic proximity and phylogeny predict elasticities and damping ratio. However, plant growth form affects which vital rates are most important for population growth (Enright *et al.*, 1995; Franco & Silvertown, 2004; Salguero-Gómez *et al.*, 2016). Further, we expect that in general species which are closely related are more likely to have the same growth form, although there are exceptions (Mack, 2003; Salguero-Gómez *et al.*, 2016). Thus, we expect that the elasticity structure of a population will be predicted by its close relatives. Higher damping ratios (index of the rate that populations return to an equilibrium after disturbance) are expected to be advantageous in more frequently disturbed environments (Stott *et al.*, 2011). Supporting this conjecture, sensitivities of λ to vital rates (closely related to elasticities) have been shown to have a high phylogenetic signal (Burns *et al.*, 2010). Because disturbance frequency can be spatially corre-

lated (Fox *et al.*, 2008; Premoli & Kitzberger, 2005), we expect the damping ratio to be predicted by geographically near populations.

Here we examine how transferable these four demographic metrics are across space and phylogeny. We also estimate how far, on average, these demographic measures can be extrapolated. Using the largest dataset of geolocated demographic models currently available, we show that while demographic metrics are predictable to some extent using neighbouring populations and related species, caution must be used in extrapolating demographic data.

MATERIALS AND METHODS

We tested the cross-population, cross-species generalisability of four different aspects of population performance using matrix population models (matrix models, hereafter) from the COMPADRE Plant Matrix Database (COMPADRE henceforth; Salguero-Gómez *et al.* 2015). This version of COMPADRE (obtained 24th October 2014) is included in Appendix 1, Supporting Information. The current version of COMPADRE Plant Matrix database is available at <http://www.compadre-db.org/Data/Compadre>.

We used a set of selection criteria to choose matrix models from the 5,672 obtained from COMPADRE to allow fair comparisons and to ensure the same set of predictor variables were available for each matrix model. Briefly, matrix models had to (i) be parameterised with at least three years of data to enable assessment of temporal variability, (ii) have GPS coordinates in COMPADRE reported to at least arc minute precision so that the location of each population could be matched up with climatic variables, (iii) have a dimension of at least 3×3 to appropriately account for individual heterogeneity (Salguero-Gómez *et al.*, 2016), (iv) be based on field data that had not been purposefully manipulated so as to examine demographic performance under unmanipulated conditions (to reduce variability unrelated to natural environmental gradients), and (v) be from 'herbaceous perennial', 'tree', 'palm', 'shrub' and 'succulent' species. We did not include annuals as their matrix models are based on a shorter temporal reference (i.e. months, seasons) than perennials, where matrix models are built on annual transi-

tions. Further details on matrix model selection are described in Appendix 2. These criteria resulted in 550 matrix models for our analysis, covering 210 plant species from 156 genera and 66 families (Table S1, Appendix 2), with populations from tropical regions to the high latitudes (Figure 1a).

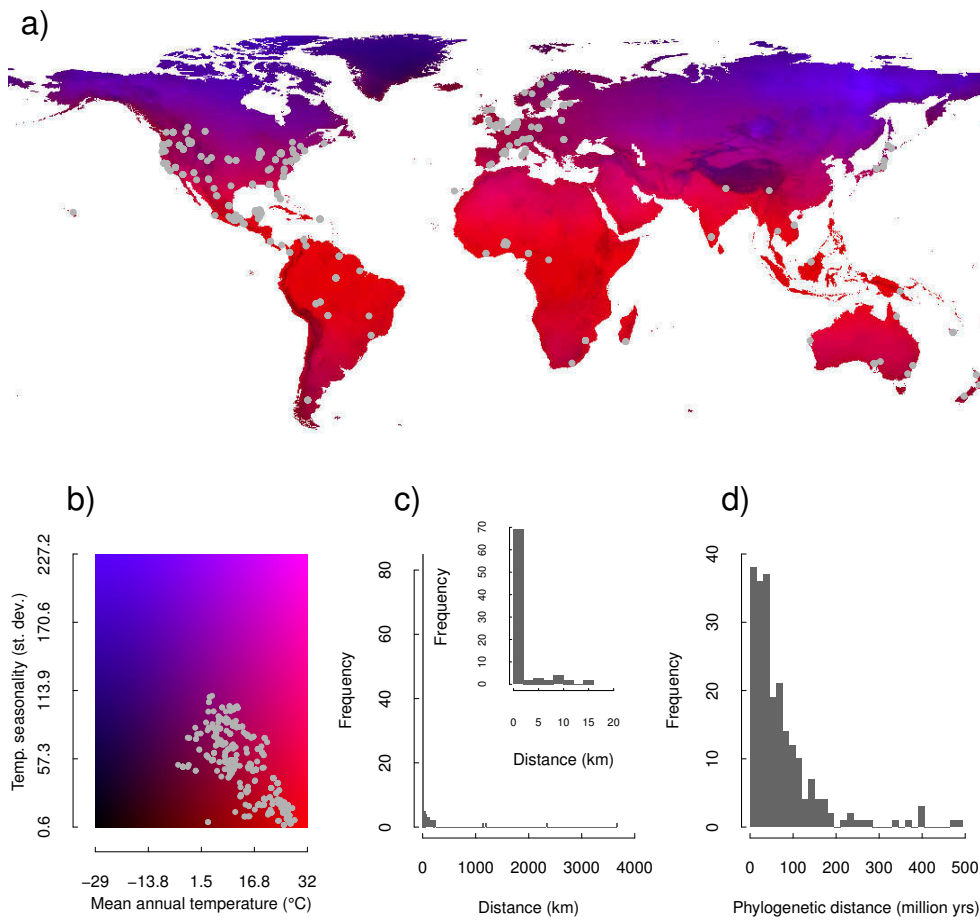


Figure 1. Locations of the 550 populations used in the analysis plotted on, a) world map coloured with mean annual temperature (°C) and temperature seasonality (standard deviation over year). Redder areas are warm and non-seasonal (i.e. tropics), blue areas are cold and seasonal, purple areas are warm and seasonal (continental temperate), and dark areas are cold and non-seasonal. b) Populations plotted on to this temperature environmental space. c) Frequency distribution of maximum between-population distance within each of the 112 species (out of 210 total), that were represented by more than one population in our dataset. Bins are 25km wide in larger plot and 2km wide in the inset. d) Phylogenetic distance (in millions of years since last common ancestor) between each of the 210 species in the dataset and the closest relative to that species in the dataset. Bins are 15 million years wide.

The demographic data are confounded in three different ways. First, some matrix models were built with data from almost the same geographic location and those populations are likely to experience similar environmental conditions (Figure 1c). Secondly, some species have closer phylogenetic relationships to others, thus, any demographic signatures that may be due to phylogenetic constraints must be separated from those that are due to environmental filtering (Blomberg & Garland, 2002). Further, populations of the same species tended to be at similar geographic locations. Of the 112 species in our dataset that were represented by more than one population, over half (70) had a maximum distance between populations ≤ 2 km, and all but five had a maximum distance between populations ≤ 100 km (Figure 1c). Finally, most (92% of species) of the matrix models for a given species come from a single study. Thus, geographic location, phylogeny and methodological differences between studies are all confounded to some extent, necessitating careful modelling of the data and cautious interpretation of results.

Metrics of demographic performance

We test the transferability of four fundamental metrics of short- and long-term population performance: asymptotic population growth rate, λ , its coefficient of variation through time, $CV(\lambda)$, the damping ratio, ρ , and a composite axis of matrix element elasticities, the Stasis-Progression Gradient (hereafter SPG).

The population growth rate, λ , is an index of how a population is projected to grow ($\lambda > 1$) or decline ($\lambda < 1$) in the long-term, if the a/biotic conditions under which the population was studied do not change (Caswell, 2001). λ is one of the most widely used demographic metrics when assessing population performance and extinction risk (Tuljapurkar & Orzack, 1980; Caswell, 2001; Ramula *et al.*, 2008; Buckley *et al.*, 2010; Crone *et al.*, 2011). The coefficient of variation in λ indicates how much population performance varies interannually. Greater $CV(\lambda)$ is expected to increase local extinction risk (Lande & Orzack, 1988; Fieberg & Ellner, 2001). Note that $CV(\lambda)$ does not, in general, inform on the realized temporal variation in population growth rate, because populations are unlikely to be at their stable stage distribution over the entire measurement period (Williams *et al.*, 2011).

The damping ratio, ρ , is an index of the rate that a population converges to its stable age or stage distribution after it has been perturbed (Stott *et al.*, 2011), and it has important implications for conservation (Koons *et al.*, 2005; Stott *et al.*, 2011). Values of λ and ρ for each matrix model were calculated with the 'popbio' R package (Stubben & Milligan, 2007).

Matrix element elasticities of λ are the proportional changes in λ caused by small proportional changes in corresponding matrix elements (Caswell, 2001). Elasticities indicate the relative importance of the demographic transitions of stasis, progression and retrogression, as well as the *per capita* contributions from sexual reproduction, to λ (de Kroon *et al.*, 1986). After the population growth rate, elasticities are the most commonly used demographic metric in plant population studies (Franco & Silvertown, 2004; Ramula *et al.*, 2008). This is especially true in conservation and invasion biology where stages and demographic processes with the highest elasticities are typically targeted for conservation across wider areas and similar species (Silvertown *et al.*, 1996; Shea & Kelly, 1998; Ramula *et al.*, 2008).

In order to compare matrix element elasticities of λ across populations and species, we classified each matrix element as belonging to the process of reproduction (both asexual and sexual), progression, stasis or retrogression (Silvertown *et al.*, 1993), producing a vector of four elasticities. Because these four elasticities must add up to one (de Kroon *et al.*, 1986), a higher value for one necessitates a lower value for the others. To overcome this limitation, we used Principal Components Analysis (PCA) to reduce the four elasticities to a single axis, PC1, which accounted for 59% of the variance. We term this axis the Stasis-Progression Gradient, SPG. At high SPG scores elasticities of λ to stasis transitions are large (loading 0.65), and elasticities of λ to reproduction and progression transitions are small (loadings -0.48 and -0.56 respectively). The opposite applies to populations with low SPG scores (see Appendix 3, Table S1 for loadings and variance explained by each axis).

Values of λ_n , ρ_n and SPG_n are derived from \mathbf{M}_n , the n^{th} mean matrix model in our dataset, where each element is the arithmetic mean of the transition rate over the study period. $\text{CV}(\lambda)_n$ was calculated from several individual matrix models (between 3 and 51), each built using data for a single annual transition. Of the 550 matrix models in our dataset, 306 reported matrix models for each year separately allowing us to calculate coefficient of variation in λ across years.

Predictors of demographic performance

We explained variation in these four demographic metrics of population performance using climate, demographic performance at neighbouring locations, and performance in related species, along with matrix model and species level attributes. The location of each matrix model is given by GPS coordinates recorded in COMPADRE, which are sourced from publications or through personal communication with the authors (R. Salguero-Gómez, unpubl. data). GPS locations were used to calculate the distance between data collection sites and to extract 16 climatic variables from the BioClim database (bio_1, bio_3 - bio_9, bio_12 - bio_19; www.worldclim.org/bioclim) along with an Aridity index from CGIAR-CSI (<http://www.csi.cgiar.org>). These variables cover different aspects of the mean and seasonal variability of temperature and precipitation, for more details see Table S3, Appendix 4. Climate predictors were extracted from raster files with 30 arc-second resolution. For each location we averaged each climatic variable over a 2km buffer zone to reduce the effect of uncertainty in study location.

Because the eight temperature variables (Table S3, Appendix 4) were highly correlated with each other we created one composite temperature variable using a Principal Component Analysis (PCA) with the `prcomp` function of the 'stats' R library (R Core Team, 2013). The first PC axis, which we refer to as PC_temp, explains 71% of the variance in temperature variables and represents a gradient from cooler seasonably variable temperate climates to hot, non-seasonal tropical climates (see Appendix 3 for more details). The Aridity Index (AI) is positively correlated with all the other precipitation variables in BioClim (Appendix 4, Table S4), except for precipitation seasonality (bio_15; Figure S1d, Appendix 3). Thus, we selected Aridity Index and bio_15 to describe precipitation at each location. We log-transformed AI because we expect small absolute differences in water availability have larger effects on population vital rates when water is a limiting factor (i.e. arid areas) (Levine *et al.*, 2008).

We measured phylogenetic relatedness, $t_{i,n}$, as millions of years since the last common ancestor of species described by matrix models \mathbf{M}_i and \mathbf{M}_n . We used the phylogeny supplied with COMPADRE (Appendix S5; Salguero-Gómez *et al.* 2015). Phylogenetic relatedness was calculated with the 'cophenetic' function from the 'stats' R package (R Core Team, 2013). We measured the

geographic distance, $d_{i,n}$, as the shortest great arc distance between the locations of matrix models \mathbf{M}_i and \mathbf{M}_n , using the 'Ellipsoidal.Distance' function in the 'GEOmap' R package (Lees, 2015).

To test if life history traits or matrix model attributes were correlated with demographic performance we used matrix dimension, species' growth form and mean life expectancy as predictors. Growth form and mean life expectancy have life history trade-off implications that may be reflected in the demographic metrics we test (Silvertown *et al.*, 1993; Enright *et al.*, 1995; Salguero-Gómez & Plotkin, 2010; Stott *et al.*, 2011). Matrix dimension has also been shown to affect the calculation of demographic metrics like ρ and elasticities (Enright *et al.*, 1995; Salguero-Gómez & Plotkin, 2010; Stott *et al.*, 2010). The 'GrowthType' variable retrieved from COMPADRE was used to classify species as either herbaceous or non-herbaceous (trees, palms, shrubs, succulents), as non-herbaceous growth forms apart from trees did not have a large enough sample size to fit them individually. At the population level, the fundamental matrix method was used to derive mean life expectancy conditional on having germinated, from each mean matrix (Caswell, 2001, pp. 120). We used the matrix dimension extracted from COMPADRE. See Table S5, Appendix 4 for the list of predictors.

The predictor and response variables in the statistical models occur at three hierarchical levels, as shown in Box 1. Briefly, phylogeny, matrix dimension and growth type are defined at the species level; the four demographic metrics, geographic location, mean life expectancy and the environmental variables are defined at the matrix model level; finally variation in population growth rate over time is based on population matrix models constructed with data from annual transitions.

Box 1. We use statistical models to explain variation in four demographic metrics (response variables) using environmental and species level predictors, along with neighboring populations and related species. Response and predictor variables in our statistical models are defined at three hierarchical levels:

Species Predictors defined at the species level <ul style="list-style-type: none"> • Phylogeny is defined at the species level, and thus the phylogenetic predictor term, Φ, is defined at the species level. • Growth type 	
Matrix model Each species is represented by one or more matrix models	
Responses defined at the matrix model level <ul style="list-style-type: none"> • Pop. growth rate, λ • Coefficient of variation in λ across time, $CV(\lambda)$ • Damping ratio, ρ • Stasis progression gradient, SPG 	Predictors defined at the matrix model level <ul style="list-style-type: none"> • Geographic location is defined for each matrix model, and thus the geographic predictor term, Ψ, is defined at the matrix model level. • Mean life expectancy • Matrix dimension • Aridity index • Precip. seasonality • Temperature
Transitions Each matrix model is based on transition rates from at least 3 years (two observed transitions)	
The response variable $CV(\lambda)$ is based on population growth rates calculated from each annual transition matrix	

Statistical analyses

We predicted transformed demographic metrics ($\ln(\lambda_n)$, $\ln(CV(\lambda)_n + 1)$, $\ln(\rho_n)$, SPG_n) using a spatially and phylogenetically lagged, linear model (Ward & Gleditsch, 2008). We transformed the demographic metrics to improve their error distributions and model fitting. Parameters were estimated in a Bayesian framework using MCMC sampler JAGS 3.4.0-1. Models were fit in R (R Core Team, 2013) using the 'R2jags' interface. The specific details of the MCMC sampling changes slightly from model to model but in general we use three chains of 100,000 samples each, thinned to take every 100th sample, with a burn in of 50,000 samples (Appendix 1).

We define our model as

$$Y_n \sim N(\mu_n, \sigma_a) \quad (1a)$$

$$\mu_n = \beta_0 + \boldsymbol{\beta}\mathbf{X}_n + \theta_p\Phi_n + \theta_g\Psi_n \quad (1b)$$

where Y_n is the predicted value for one of the transformed demographic metrics for matrix model n , drawn from a normal distribution with a standard deviation of $\sigma_a \sim \text{Gamma}(0.0001, 0.0001)$ and a mean of μ_n . The parameter β_0 is the intercept and $\boldsymbol{\beta}$ is a column vector of slopes. Each slope corresponds to an effect size of one of the aforementioned predictors or their interactions.

$$\boldsymbol{\beta} = \begin{pmatrix} \beta_1 \\ \beta_2 \\ \vdots \\ \beta_K \end{pmatrix}$$

with K being the total number of climatic and species-level predictors in the model. There are six main effect predictors (matrix dimension, growth type, mean life expectancy, PC_temp, Aridity Index, precipitation seasonality), including two-way interactions between the main effects resulted in $K = 18$. Each slope in $\boldsymbol{\beta}$, and the intercept β_0 , were drawn from wide prior distributions, $\beta_k \sim N(0, 0.0001)$, where $N(\cdot)$ is a normal distribution. \mathbf{X} is a $K \times J$ matrix of K species-level and climatic predictors, and their interactions, for all J matrix models.

To capture the effect of phylogeny and geographic location, we included a phylogenetic predictor term $\theta_p\Phi_n$, and a geographic predictor term $\theta_g\Psi_n$, respectively (Eq. 2). The terms $\theta_p\Phi_n$ and $\theta_g\Psi_n$ predict the value of Y_n as a weighted average of matrix model n 's relatives or neighbours respectively.

$$\Phi_n = \frac{\sum_{\forall i \neq n} Y_i \exp[-\phi t_{i,n}]}{\sum_{\forall i \neq n} \exp[-\phi t_{i,n}]} \quad (2a)$$

$$\Psi_n = \frac{\sum_{\forall i \neq n} Y_i \exp[-\psi d_{i,n}]}{\sum_{\forall i \neq n} \exp[-\psi d_{i,n}]} \quad (2b)$$

where $\phi \sim \text{Unif}(0, 1)$ (see Appendix 1 for minor modifications to these limits) modulates how phylogenetically close *vs.* distant relatives contribute to

predicting Y_n . Similarly $\psi \sim \text{Unif}(0, 1)$ controls how geographically near *vs.* distant neighbours contribute to predicting Y_n . When ϕ or ψ are 0, all populations contribute equally to the prediction of Y_n regardless of distance, either phylogenetic or geographic; as ϕ or ψ increase, more closely related species, or geographically closer locations, have a greater contribution to the prediction of Y_n . The term $t_{i,n}$ is the phylogenetic distance between species represented by matrix models i and n . $d_{i,n}$ is the geographic distance between the locations of matrix models i and n . $\theta_p \sim N(0, 0.0001)$ and $\theta_g \sim N(0, 0.0001)$ are coefficients that scale the phylogenetic and geographic predictions. Any explanatory power from the geographic and phylogenetic predictor terms is a result of spatial auto-correlation in both measured and unmeasured environmental variables and phylogenetically conserved functional traits, rather than distance *per se*. If demographic attributes are random with respect to spatially auto-correlated environmental factors, or are not phylogenetically constrained, the phylogenetic and geographic and predictor terms (Φ , and Ψ respectively) will explain none of the variance in the four demographic metrics tested.

Study, species and location are all to some extent confounded, due to many populations of the same species being from the same study and similar geographic locations. To test the effect this had on the performance of our models, we also tested models where the spatial and phylogenetic predictor terms were based on a reduced, but less confounded set of neighbours and relatives. We ran models where Y_i in the geographic and phylogenetic prediction terms (Eq. 2) were only based on matrix models from different locations (that is, where $d_{i,n} \neq 0$) or which were based on a different species (*i.e.* where $t_{i,n} \neq 0$). We call these 'no_self' models. In addition, we tested five combinations of predictors so that the explanatory power of simplified models could be tested. This led to eight different modifications of the general model (Eq. 1), detailed in Table 1. These model versions were used to predict the four demographic metrics outlined above, resulting in a total of 32 separate models.

Table 1. Statistical models used to predict the four demographic metrics, population growth rate, its temporal variation, damping ratio and the composite elasticities, Stochastic Progression Gradient (SPG). Because the environmental and species level predictors (matrix dimension, growth type, mean life expectancy, first principal component of the temperature variables (PC_temp), Aridity Index, precipitation seasonality) are spatially autocorrelated the 'main_int' and 'main' models were only fit using geographic and phylogenetic predictor terms based on all 550 matrix models in our dataset.

model name	environmental and species level predictors	phylogenetic predictor	geographic predictor
main_int	All six main effects and 2-way interactions, giving 18 terms		Based on all populations
main	Only the six main effects		Based on all populations
phygeo-all_pops	Not included		Based on all populations
phygeo-no_self	Not included	Based only on populations that were not of the same species	Based only on populations that were not in the same location
phy-all_pops	Not included	Based on all populations	Not included
phy-no_self	Not included	Based only on populations that were not of the same species	Not included
geo-all_pops	Not included	Not included	Based on all populations
geo-no_self	Not included	Not included	Based only on populations that were not in the same location

Since geographic location was used to define our climatic predictors, those predictors were geographically and phylogenetically correlated. Thus, we carefully examined the simplification of the general model in Eq. 1. Models that contained environmental and species level predictors (*i.e.* 'main_int' and 'main', see Table 1 for model names) also had to include the geographic and phylogenetic predictor terms based on all populations (as opposed to the 'no_self' geographic and phylogenetic predictor term). When running 'no_self' models containing environmental and species-level predictors we could not know if any significantly non-zero coefficients in β represented a real effect, or if that predictor was simply acting as a poor proxy for geo-

graphic location. This raises the general point that these are phenomenological models which find patterns in the data, patterns which are likely to be caused by multiple related processes acting simultaneously.

RESULTS

None of the environmental, species- or matrix model level variables had a significant effect on the demographic metrics tested (λ , $CV(\lambda)$, ρ , and SPG) over and above the effect of the geographic and phylogenetic predictor terms. All of the credible intervals on the coefficients in β , Eq. 1 encompass 0. This is further illustrated by Figure 2, where the full model containing all the predictors did not explain much more variance in any of the demographic metrics than the model that only contained the predictor terms based on geographic and phylogenetic distance (phygeo-allpops). For this reason we do not report results for the 'main' model as it produced the same results as the 'main_int' and 'phygeo-all_pops' models. The 'phygeo' also had the lowest (or equal lowest) DIC values (Figure 2), suggesting that having both geographic and phylogenetic predictor terms was a good trade-off between parsimony and explanatory power. Overall, models including only predictor terms based on phylogenetic or geographic distance had R^2 values between 20% and 65% depending of the demographic metric (Figure 2). This explanatory power suggests that some environmental and species level factors had important effects on population performance. See diagnostic plots in Appendix 1 for full breakdown of credible intervals and model performance (Appendix_1_analysis_pipeline/Appendix_1_model_code_and_plotting/pre-run_model_output).

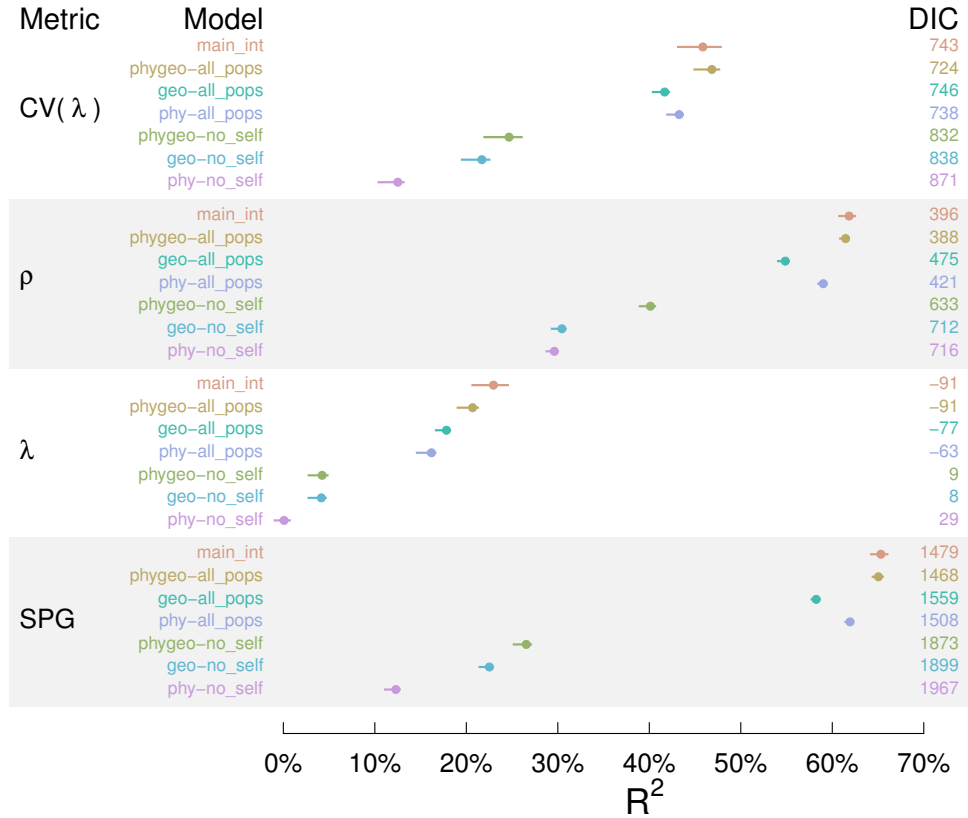


Figure 2. We use geographically and phylogenetically lagged statistical models to explain the variance in four key demographic metrics. We use R^2 to quantify explanatory power, higher values indicate more variance explained. Median R^2 (points) and 95% (solid lines) quantiles were taken across 1,500 MCMC samples. Deviance Information Criteria (DIC) is an index of model performance penalized by the number of parameters. Lower DIC numbers indicate more parsimonious models that performed well relative to the other models tested. Note that DIC cannot be compared between metrics, or between 'all_pops' and 'no_self' models for the same metric. Colour indicates the model structure. See Table 1 for definitions of 'main_int', 'phygeo', 'geo' and 'phy' models, and the difference between models with spatial and phylogenetic prediction terms based 'all_pops' and 'no_self' predictions.

The best models had R^2 values around 65%, however care must be taken not to over interpret the predictive power of these models. In models where the geographic and phylogenetic prediction terms were fit using all populations the effect of species, local environment and study methodology are confounded. To test how much of an effect this had on the explanatory power of our models we fitted 'no_self' models (Table 1). Even after these self pre-

dictions were removed several of the 'no_self' models still explained 20-40% of variation in the metrics of demographic performance (Figure 2).

Our models explained more variation in some metrics of population performance than others; with relatively high explanatory power for a matrix model's position on the SPG continuum and damping ratio (ρ), and lower explanatory power for asymptotic population growth rate (λ) and its temporal variation. The best models explained around 65% of the variation in SPG and damping ratio ('main_int', 'main' and 'phygeo-all_pops' density distributions 2) and only 25-45% of variation in $CV(\lambda)$ and λ . The 'no_self' models explained between 12-25% of the variation in SPG, 40% of the variation in damping ratio, 5% of the variation population growth rate (λ), and 15-25% of variation in $CV(\lambda)$ (Figure 2).

For all demographic metrics, except ρ , the spatial term explained more variation than the phylogenetic term (Figure 2). The 'no_self' models with only a spatial term explain almost as much variation as models with both a geographic and phylogenetic prediction term (phygeo-no_self in Figure 2). In contrast 'no_self' models with only a phylogenetic term typically had an R^2 about half that of the model including both spatial and phylogenetic terms. Thus, both the spatial and phylogenetic terms are explaining much of the same variance in the response, with the spatial term explaining some variance not explained by phylogenetic term.

To examine the way predictive support drops off with geographic and phylogenetic distance, we plotted the negative exponential decay models that underpin the geographic and phylogenetic prediction terms (Eq. 2). Here we present decay curves for the 'phygeo-no_self' model (Table 1), since this model had the lowest DIC of the 'no_self' models. Results were similar across different models, although uncertainty around the decay curves varies greatly between models (Appendix 5). For models predicting population growth rates (λ) and SPG virtually all predictive support came from locations that were within 15 km of the target location (Figure 3a,c). Predictive support for $CV(\lambda)$ and damping ratio (ρ) came from locations within 35 km (Figure 3b,d). Predictive support based on phylogeny came from species that diverged <100 mya for SPG, < 20 mya for $CV(\lambda)$ and < 10 mya for λ and ρ (Figure 3).

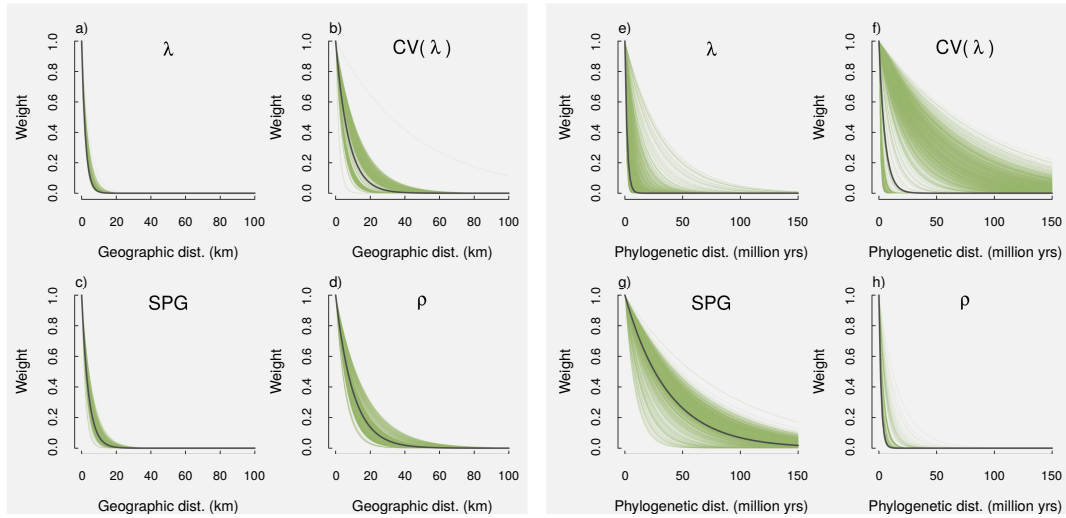


Figure 3. Decay curves are the basis of the geographic and phylogenetic predictor terms, and show how quickly predictive support from neighbouring locations or other species declines with distance (either geographic or phylogenetic). Decay curves for geographic (a-d) and phylogenetic (e-h) predictor terms for each metric, population growth rate (λ), its temporal variation ($CV(\lambda)$), Stasis Progression Gradient (SPG) and damping ratio (ρ). The model presented here, phygeo-no_self, has no fixed effects, and predictions were based on geographic locations and species that were different to that being predicted for. Lines show the curve produced by the estimated decay parameter for each of the 1,500 MCMC samples. Grey lines depict the average curve. Average decay curves for other models are generally similar, although the uncertainty around decay curve can vary greatly between different models for the same measure. Decay plots for all other models can be found in Appendix 5.

DISCUSSION

Important aspects of plant population performance, data which are time-consuming and expensive to collect for each population, can be inferred from nearby locations and, to a lesser extent, from related species. Even after removing predictions from the same location or the same species, we can still explain 25%-40% of the variation in damping ratio, elasticities and temporal variation in population growth rate. However, our results also suggest that there are important limits to generalising population performance across geographic locations and between species.

It is common practice in demography, applied ecology and conservation to measure the demography of a species in a few locations and then apply that understanding to the species over a much wider region (Shea & Kelly, 1998; Doak *et al.*, 2005; Crone *et al.*, 2011; Sæther *et al.*, 2005; Salguero-Gómez *et al.*, 2016). In contrast, we often expect considerable geographic variation in demographic performance of populations within species (e.g., Jongejans & de Kroon 2005, Merow *et al.* 2014). In our dataset, species and geographic location are too confounded to directly test how transferable demographic information is within species because most populations of the same species were geographically close to each other. However, in our analysis using a dataset of unprecedented size in comparative plant demography, closely related species were much weaker predictors of population performance than geographically close populations. The explanatory power of the geographic predictor term suggests that something about the mid to small-scale environment is predictive of demography, specifically elasticities of population growth rate, damping ratio and temporal variation in population growth rate. Mid- to small-scale environmental variables will likely include many local drivers beyond climate, such as soil, anthropogenic impacts (Cole *et al.*, 2014), disturbances and biotic interactions (Silvertown *et al.*, 1996; Thuiller *et al.*, 2014). It is this mid to small-scale signal that is often lost with global comparisons (Salguero-Gómez *et al.*, 2016).

Borrowing information across closely related species may be more useful for some aspects of demography than others (Blomberg & Garland, 2002). The phylogenetic term unambiguously explained around 10% of the variance in damping ratio over and above the variance explained by the geographic predictor term, much more than the other three demographic metrics. In the case of the damping ratio, only species that diverged < 10 mya provided good support for predicting the damping ratio of another species. In our dataset 38 genera were represented by two or more species; of these eight had at least one species pair that diverged < 15 mya, and three had species that diverged from each other < 10 mya. This suggests that, in our dataset at least, it is uncommon for species in the same genus to have diverged recently enough to help explain variation in each others damping ratio.

Why we were able to explain so much variation in damping ratio remains an open question. It has been suggested that damping ratio is strongly influenced by a limited set of traits and life history strategies (e.g. resprouting) that help plant populations recover from, or take advantage of, disturbances

(Pausas & Lavorel, 2003; Clarke *et al.*, 2010). In contrast the other three demographic metrics are strongly influenced by multiple environmental and biotic factors (Silvertown *et al.*, 1996), each of which will introduce noise into the prediction. Further, populations at their stable stage distribution can show up to a 16-fold difference in population growth rate compared to those that have been perturbed (Williams *et al.*, 2011). Given this large difference in population performance, it is likely that traits and demographic strategies which affect the time taken to return to the stable stage distribution (measured by damping ratio) are under strong selective pressure (Lamont & Downes, 2011), resulting in a high phylogenetic signal (Blomberg & Garland, 2002). In addition, variability in environmental conditions are spatially correlated (Fox *et al.*, 2008; Premoli & Kitzberger, 2005), and thus we might expect disturbance driven demography to be more spatially predictable.

An important caveat to our analysis is that most species were represented in our dataset by a single location - although we used the most extensive database of plant demography available (Salguero-Gómez *et al.*, 2015). This means that the decay curves are averages across many different species and habitats, and could be different for any given species or location (Diez *et al.*, 2014). Geographic location and phylogeny are confounded to some extent in our dataset and some of the signal in the geographic decay curves may be due to phylogenetic signal. We can however see that the geographic predictor term in our analysis does explain variation in the demographic metrics that cannot be explained by the phylogenetic term. Our analysis did not show which environmental and species level variables are driving the explanatory power of the geographic and phylogenetic predictor terms. Even those variables we included as predictors were highly spatially auto-correlated, and so could have contributed to the explanatory power of the geographic predictor term. The effect of climatic variables that vary at scales smaller than the accuracy of study locations (e.g. soil properties) will be impossible to test using comparative methods. Likewise, we could not say much about the effect of growth type, aside from herbaceous perennials, due to the small sample size of trees, palms and succulents. To get an understanding of the drivers of demography across space and species, and whether the same drivers are common between species and locations, we need to sample multiple species, at multiple locations, at different scales.

Despite these caveats, our dataset covered a large number of species and environments and the general results are clear: we can generalise from in-

dividual demographic studies. However, even with the largest geo-located dataset of demographic studies available we can only justify extrapolating important aspects of demography at limited scales, especially compared to the scales that threats such as species invasions and climate change occur at. Thus, the initial assumption should be that any demographic results we obtain are applicable to the population they were measured for and those in the immediate environment. This does not mean that we will never be able to extrapolate demographic results, but more spatially extensive sampling is needed to understand how population performance changes between species and in response to environmental drivers.

ACKNOWLEDGEMENTS

SRC was supported by the ARC Center of Excellence in Environmental Decisions and Trinity College Dublin. RS-G was supported by a DE140100505 grant of the Australian Research Council and a NERC IRF (R/142195-11-1). YMB was supported in part by a research grant from Science Foundation Ireland (SFI) under Grant Number 15/ERC/D/2803 and a Marie-Curie Career Integration Grant. We thank the Max Planck Institute for Demographic Research for support in the development of and access to the COMPADRE Plant Matrix Database.

SUPPORTING INFORMATION

Appendix 1: Statistical analysis and plotting scripts
Appendix 2: Selection criteria applied to COMPADRE Plant Matrix Database
Appendix 3: PCA loadings and variance explained by each axis
Appendix 4: Environmental variables and predictors used in the analysis
Appendix 5: Phylogenetic and geographic decay curves for all models and demographic metrics

References

1. Blomberg, S.P. & Garland, T. (2002). Tempo and mode in evolution: phylogenetic inertia, adaptation and comparative methods. *Journal of Evolutionary Biology*, 15, 899–910.
2. Buckley, Y.M., Ramula, S., Blomberg, S.P., Burns, J.H., Crone, E.E., Ehrlén, J., Knight, T.M., Pichancourt, J.B., Quested, H. & Wardle, G.M. (2010). Causes and consequences of variation in plant population growth rate: a synthesis of matrix population models in a phylogenetic context. *Ecology Letters*, 13, 1182–1197.
3. Burns, J.H., Blomberg, S.P., Crone, E.E., Ehrlén, J., Knight, T.M., Pichancourt, J.B., Ramula, S., Wardle, G.M. & Buckley, Y.M. (2010). Empirical tests of life-history evolution theory using phylogenetic analysis of plant demography. *Journal of Ecology*, 98, 334–344.
4. Caswell, H. (2001). *Matrix population models: Construction, analysis and interpretation*. 2nd edn. Sinauer Associates Inc., Sunderland, MA, USA.
5. Clarke, P.J., Lawes, M.J. & Midgley, J.J. (2010). Resprouting as a key functional trait in woody plants—challenges to developing new organizing principles. *New Phytologist*, 188, 651–654.
6. Cole, E.M., Bustamante, M.R., Almeida-Reinoso, D. & Funk, W.C. (2014). Spatial and temporal variation in population dynamics of andean frogs: Effects of forest disturbance and evidence for declines. *Global Ecology and Conservation*, 1, 60–70.
7. Crone, E.E., Menges, E.S., Ellis, M.M., Bell, T., Bierzychudek, P., Ehrlén, J., Kaye, T.N., Knight, T.M., Lesica, P., Morris, W.F. *et al.* (2011). How do plant ecologists use matrix population models? *Ecology Letters*, 14, 1–8.
8. Diez, J.M., Giladi, I., Warren, R. & Pulliam, H.R. (2014). Probabilistic

- and spatially variable niches inferred from demography. *Journal of ecology*, 102, 544–554.
9. Doak, D.F., Gross, K. & Morris, W.F. (2005). Understanding and predicting the effects of sparse data on demographic analyses. *Ecology*, 86, 1154–1163.
 10. Doak, D.F. & Morris, W.F. (2010). Demographic compensation and tipping points in climate-induced range shifts. *Nature*, 467, 959–962.
 11. Ehrlén, J. & Morris, W.F. (2015). Predicting changes in the distribution and abundance of species under environmental change. *Ecology Letters*, 18, 303–314.
 12. Enright, N., Franco, M. & Silvertown, J. (1995). Comparing plant life histories using elasticity analysis: the importance of life span and the number of life-cycle stages. *Oecologia*, 104, 79–84.
 13. Fieberg, J. & Ellner, S.P. (2001). Stochastic matrix models for conservation and management: a comparative review of methods. *Ecology Letters*, 4, 244–266.
 14. Fox, J.C., Bi, H. & Ades, P.K. (2008). Modelling spatial dependence in an irregular natural forest. *Silva Fennica*, 42, 35.
 15. Franco, M. & Silvertown, J. (2004). A comparative demography of plants based upon elasticities of vital rates. *Ecology*, 85, 531–538.
 16. Gerst, K.L., Angert, A.L. & Venable, D.L. (2011). The effect of geographic range position on demographic variability in annual plants. *Journal of Ecology*, 99, 591–599.
 17. Hartmann, D., Klein Tank, A., Rusticucci, M., Alexander, L., Brönnimann, S., Charabi, Y., Dentener, F., Dlugokencky, E., Easterling, D.,

- Kaplan, A., Soden, B., Thorne, P., Wild, M. & Zhai, P. (2013). Observations: Atmosphere and surface. In: *Climate Change 2013: The Physical Science Basis. Contribution of Working Group I to the Fifth Assessment Report of the Intergovernmental Panel on Climate Change* (eds. Stocker, T., Qin, D., Plattner, G., Tignor, M., Allen, S., Boschung, J., Nauels, A., Xia, Y., Bex, V. & Midgley, P.). Cambridge University Press, Cambridge, United Kingdom and New York, USA.
18. Jongejans, E. & de Kroon, H. (2005). Space versus time variation in the population dynamics of three co-occurring perennial herbs. *Journal of Ecology*, 93, 681–692.
19. Koons, D.N., Grand, J.B., Zinner, B. & Rockwell, R.F. (2005). Transient population dynamics: relations to life history and initial population state. *Ecological Modelling*, 185, 283–297.
20. de Kroon, H., Plaisier, A., van Groenendael, J. & Caswell, H. (1986). Elasticity: the relative contribution of demographic parameters to population growth rate. *Ecology*, 67, 1427–1431.
21. Lamont, B.B. & Downes, K.S. (2011). Fire-stimulated flowering among resprouters and geophytes in australia and south africa. *Plant Ecology*, 212, 2111–2125.
22. Lande, R. & Orzack, S.H. (1988). Extinction dynamics of age-structured populations in a fluctuating environment. *Proceedings of the National Academy of Sciences of the United States of America*, 85, pp. 7418–7421.
23. Lees, J.M. (2015). *GEOmap: Topographic and Geologic Mapping*. R package version 2.3-5.
24. Levine, J.M., McEachern, A.K. & Cowan, C. (2008). Rainfall effects on rare annual plants. *Journal of Ecology*, 96, 795–806.
25. Mack, R.N. (2003). Phylogenetic constraint, absent life forms, and

- preadapted alien plants: a prescription for biological invasions. *International Journal of Plant Sciences*, 164, S185–S196.
26.
McGeoch, M.A., Butchart, S.H.M., Spear, D., Marais, E., Kleynhans, E.J., Symes, A., Chanson, J. & Hoffmann, M. (2010). Global indicators of biological invasion: species numbers, biodiversity impact and policy responses. *Diversity and Distributions*, 16, 95–108.
27.
Merow, C., Latimer, A.M., Wilson, A.M., McMahon, S.M., Rebelo, A.G. & Silander, J.A. (2014). On using integral projection models to generate demographically driven predictions of species' distributions: development and validation using sparse data. *Ecography*, 37, 1167–1183.
28.
Pausas, J.G. & Lavorel, S. (2003). A hierarchical deductive approach for functional types in disturbed ecosystems. *Journal of Vegetation Science*, 14, 409–416.
29.
Premoli, A.C. & Kitzberger, T. (2005). Regeneration mode affects spatial genetic structure of *nothofagus dombeyi* forests. *Molecular Ecology*, 14, 2319–2329.
30.
R Core Team (2013). *R: A Language and Environment for Statistical Computing*. R Foundation for Statistical Computing, Vienna, Austria.
31.
Ramula, S., Knight, T.M., Burns, J.H. & Buckley, Y.M. (2008). General guidelines for invasive plant management based on comparative demography of invasive and native plant populations. *Journal of Applied Ecology*, 45, 1124–1133.
32.
Sæther, B.E., Engen, S., Møller, A.P., Visser, M.E., Matthysen, E., Fiedler, W., Lambrechts, M.M., Becker, P.H., Brommer, J.E., Dickinson, J. *et al.* (2005). Time to extinction of bird populations. *Ecology*, 86, 693–700.
33.
Salguero-Gómez, R., Jones, O.R., Archer, C.R., Bein, C., Buhr, H., Farack,

- C., Gottschalk, F., Hartmann, A., Henning, A., Hoppe, G. *et al.* (2016). Comadre: a global data base of animal demography. *Journal of Animal Ecology*.
34. Salguero-Gómez, R., Jones, O.R., Archer, C.R., Buckley, Y.M., Che-Castaldo, J., Caswell, H., Hodgson, D., Scheuerlein, A., Conde, D.A., Brinks, E. *et al.* (2015). The COMPADRE plant matrix database: an open online repository for plant demography. *Journal of Ecology*, 103, 202–218.
35. Salguero-Gómez, R. & de Kroon, H. (2010). Matrix projection models meet variation in the real world. *Journal of Ecology*, 98, 250–254.
36. Salguero-Gómez, R. & Plotkin, J.B. (2010). Matrix dimensions bias demographic inferences: implications for comparative plant demography. *The American Naturalist*, 176, 710–722.
37. Salguero-Gómez, R., Jones, O.R., Jongejans, E., Blomberg, S.P., Hodgson, D.J., Mbeau-Ache, C., Zuidema, P.A., de Kroon, H. & Buckley, Y.M. (2016). Fast–slow continuum and reproductive strategies structure plant life-history variation worldwide. *Proceedings of the National Academy of Sciences*, 113, 230–235.
38. Shea, K. & Kelly, D. (1998). Estimating biocontrol agent impact with matrix models: *Carduus nutans* in new zealand. *Ecological Applications*, 8, 824–832.
39. Silvertown, J., Franco, M. & Menges, E. (1996). Interpretation of elasticity matrices as an aid to the management of plant populations for conservation. *Conservation Biology*, 10, 591–597.
40. Silvertown, J., Franco, M., Pisanty, I. & Mendoza, A. (1993). Comparative plant demography—relative importance of life-cycle components to the finite rate of increase in woody and herbaceous perennials. *Journal of Ecology*, pp. 465–476.

41.
Stott, I., Franco, M., Carslake, D., Townley, S. & Hodgson, D. (2010). Boom or bust? a comparative analysis of transient population dynamics in plants. *Journal of Ecology*, 98, 302–311.
42.
Stott, I., Townley, S. & Hodgson, D.J. (2011). A framework for studying transient dynamics of population projection matrix models. *Ecology Letters*, 14, 959–970.
43.
Stubben, C.J. & Milligan, B.G. (2007). Estimating and analyzing demographic models using the popbio package in r. *Journal of Statistical Software*, 22.
44.
Sutherland, W.J., Freckleton, R.P., Godfray, H.C.J., Beissinger, S.R., Benton, T., Cameron, D.D., Carmel, Y., Coomes, D.A., Coulson, T., Emmerson, M.C., Hails, R.S., Hays, G.C., Hodgson, D.J., Hutchings, M.J., Johnson, D., Jones, J.P.G., Keeling, M.J., Kokko, H., Kunin, W.E., Lambin, X., Lewis, O.T., Malhi, Y., Mieszkowska, N., Milner-Gulland, E.J., Norris, K., Phillimore, A.B., Purves, D.W., Reid, J.M., Reuman, D.C., Thompson, K., Travis, J.M.J., Turnbull, L.A., Wardle, D.A. & Wiegand, T. (2013). Identification of 100 fundamental ecological questions. *Journal of ecology*, 101, 58–67.
45.
Thuiller, W., Münkemüller, T., Schiffrers, K.H., Georges, D., Dullinger, S., Eckhart, V.M., Edwards, T.C., Gravel, D., Kunstler, G., Merow, C. *et al.* (2014). Does probability of occurrence relate to population dynamics? *Ecography*, 37, 1155–1166.
46.
Tuljapurkar, S. & Orzack, S.H. (1980). Population dynamics in variable environments i. long-run growth rates and extinction. *Theoretical Population Biology*, 18, 314–342.
47.
Villellas, J., Doak, D.F., García, M.B. & Morris, W.F. (2015). Demographic compensation among populations: what is it, how does it arise and what are its implications? *Ecology letters*, 18, 1139–1152.

48. Ward, M.D. & Gleditsch, K.S. (2008). *Spatial regression models*. vol. 155 of *Quantitative Applications in the Social Sciences*. Sage, Thousand Oaks, CA.
49. Williams, J.L., Ellis, M.M., Bricker, M.C., Brodie, J.F. & Parsons, E.W. (2011). Distance to stable stage distribution in plant populations and implications for near-term population projections. *Journal of ecology*, 99, 1171–1178.

Appendix 1: Analysis Pipeline

The data extraction, analysis code, model diagnostics and some pre-run model objects can be found at this github repository. This repository contains two folders, this first 'Appendix_1_data_extraction_processing', contains code that:

1. Takes data from the COMPADRE Plant Matrix Database (R object downloaded on the 24th of October 2014 included in file) and filters out the populations that do not meet our selection criteria.
2. Calculates the four demographic metrics we focus on, Population growth rate (λ), temporal variation of λ ($CV(\lambda)$), damping ratio (ρ) and a composite variable for elasticities of λ (SPG).
3. Extract data from BioClim (<http://worldclim.org/current>) and Aridity Index (CGIAR-CSI GeoPortal; <http://www.csi.cgiar.org>) raster layers and perform PCA analysis on the relevant variables
4. Combine all the filtered data from COMPADRE with the demographic metrics and environmental variables and saves the resulting data frame as
`'combined_bc_ai_all_responses.Rdata'`

The second folder 'Appendix_1_model_code_and_plotting' contains code that takes the data frame in 'combined_bc_ai_all_responses.Rdata' and fits statistical models using JAGS 3.4.0-1. The statistical models used in the analysis are defined in the file 'non_elast_predict_models.R'. These models are called using the 'r2jags' interface in the file 'pop_metric_prediction.R'. the resulting model objects are saved and called by 'plotting_functions.R' to produce diagnostic and trace plots for the models, along with the results plots for the paper and Appendices.

WARNING: Several steps (in particular the BioClim data extraction and the MCMC sampling) take hours, days, or weeks to run. If one were to try and run this code as is, it will take a long time. Secondly this analysis pipeline

has multiple steps, each of which requires several libraries and dependencies to work. It would be surprising if anybody could get it to work on the first attempt.

Appendix 2: Data extraction

We sourced matrix models from the COMPADRE Plant Matrix Database (Salguero-Gómez *et al.*, 2015), downloaded on the 24th of October 2014, this version is included in Appendix 1. For the most recent version of the COMPADRE Plant Matrix Database see this link). We used a set of constraining criteria to choose matrix models from the 5,672 contained in this version of COMPADRE to allow fair comparisons and to ensure the same set of predictor variables are available for each matrix model.

Each matrix had to:

1. have all relevant meta-data available, namely GPS coordinates, GrowthType, MatrixTreatment, SurvivalIssue, StudyDuration, MatrixEndYear and MatrixStartYear.
2. be parameterised with at least three years of data to enable assessment across temporal variability.
3. have GPS coordinates in COMPADRE reported to at least arc minute precision so that the location of each population could be matched up with climatic variables.
4. have a dimension of at least 3×3 to appropriately account for individual heterogeneity
5. be based on field data that had not been purposely manipulated so as to examine demographic performance under natural conditions
6. be for a species classified as 'herbaceous perennial', 'tree', 'palm', 'shrub' and 'succulent', because sample size of other growth types was too low for our allow analyses. We did not include annuals as their matrix models are based on a shorter temporal reference (i.e. months, seasons) than perennials, where matrix models are built on annual transitions.
7. be denoted as 'Divided' in the 'MatrixSplit' COMPADRE variable.
8. be denoted 'Mean' in the 'MatrixComposite' COMPADRE variable.
9. refer to a single population (i.e. not refer to more than one named population).

10. have a value ≤ 1.05 for the 'SurvivalIssue' COMPADRE variable.
11. we removed populations where the 'MatrixTreatment' COMPADRE variable indicated they were mowed, burnt or had seeds added.
12. we also removed matrices where the 'Observation' COMPADRE variable indicated there was uncertainty in the GPS coordinates or estimates of the vital rates.
13. We remove species *Chamaecrista keyensis* as it was unclear where these populations were located.
14. the species had to be in the phylogeny provided in Appendix 5 of Salguero-Gómez *et al.* (2015).
15. the location of some populations were not represented in the BioClim raster layers (often populations near coast lines), as a result environmental predictors could not be extracted for these populations and they had to be excluded from our data.

These filtering criteria are largely implemented in lines 130–155 of the file '~ / Appendix_1_data_extraction_processing / data_extraction_and_clean_up.R', Appendix 1. These criteria resulted in 550 matrix models for our analysis, covering 210 plant species from 156 genera, covering both angiosperms and gymnosperms, with populations from tropical regions to the high latitudes. The full list of species in the resulting data set is given in Table S1.

Table S1. List of species used in the analysis

Geuns-Species	Family	Order	Class	Phylum
Actaea elata	Ranunculaceae	Ranunculales	Magnoliopsida	Magnoliophyta
Actaea spicata	Ranunculaceae	Ranunculales	Magnoliopsida	Magnoliophyta
Agrimonia eupatoria	Rosaceae	Rosales	Magnoliopsida	Magnoliophyta
Agropyron cristatum	Poaceae	Poales	Liliopsida	Magnoliophyta
Alliaria petiolata	Brassicaceae	Brassicales	Magnoliopsida	Magnoliophyta
Allium tricoccum	Amaryllidaceae	Asparagales	Liliopsida	Magnoliophyta
Anemone patens	Ranunculaceae	Ranunculales	Magnoliopsida	Magnoliophyta
Anthyllis vulneraria	Leguminosae	Fabales	Magnoliopsida	Magnoliophyta
Aquilegia chrysantha	Ranunculaceae	Ranunculales	Magnoliopsida	Magnoliophyta
Boechera fecunda	Brassicaceae	Brassicales	Magnoliopsida	Magnoliophyta
Arisaema serratum	Araceae	Alismatales	Liliopsida	Magnoliophyta
Aristida bipartita	Poaceae	Poales	Liliopsida	Magnoliophyta
Armeria maritima	Plumbaginaceae	Caryophyllales	Magnoliopsida	Magnoliophyta
Artemisia genipi	Compositae	Asterales	Magnoliopsida	Magnoliophyta
Aster amellus	Compositae	Asterales	Magnoliopsida	Magnoliophyta
Astragalus michauxii	Leguminosae	Fabales	Magnoliopsida	Magnoliophyta
Astragalus scaphoides	Leguminosae	Fabales	Magnoliopsida	Magnoliophyta
Astragalus tyghensis	Leguminosae	Fabales	Magnoliopsida	Magnoliophyta
Dioscorea chouardii	Dioscoreaceae	Dioscoreales	Liliopsida	Magnoliophyta

Bouteloua rigidiseta	Poaceae	Poales	Liliopsida	Magnoliophyta
Brassica insularis	Brassicaceae	Brassicales	Magnoliopsida	Magnoliophyta
Calathea micans	Marantaceae	Zingiberales	Liliopsida	Magnoliophyta
Calathea ovandensis	Marantaceae	Zingiberales	Liliopsida	Magnoliophyta
Calochortus albus	Liliaceae	Liliales	Liliopsida	Magnoliophyta
Calochortus lyallii	Liliaceae	Liliales	Liliopsida	Magnoliophyta
Calochortus obispoensis	Liliaceae	Liliales	Liliopsida	Magnoliophyta
Calochortus pulchellus	Liliaceae	Liliales	Liliopsida	Magnoliophyta
Calochortus tiburonensis	Liliaceae	Liliales	Liliopsida	Magnoliophyta
Carduus nutans	Compositae	Asterales	Magnoliopsida	Magnoliophyta
Centaurea horrida	Compositae	Asterales	Magnoliopsida	Magnoliophyta
Actaea cordifolia	Ranunculaceae	Ranunculales	Magnoliopsida	Magnoliophyta
Cirsium acaule	Compositae	Asterales	Magnoliopsida	Magnoliophyta
Cirsium dissectum	Compositae	Asterales	Magnoliopsida	Magnoliophyta
Cirsium palustre	Compositae	Asterales	Magnoliopsida	Magnoliophyta
Cirsium pannonicum	Compositae	Asterales	Magnoliopsida	Magnoliophyta
Cirsium pitcheri	Compositae	Asterales	Magnoliopsida	Magnoliophyta
Cirsium vulgare	Compositae	Asterales	Magnoliopsida	Magnoliophyta
Cryptantha flava	Boraginaceae	Lamiales	Magnoliopsida	Magnoliophyta
Cynoglossum officinale	Boraginaceae	Lamiales	Magnoliopsida	Magnoliophyta
Cynoglossum virginianum	Boraginaceae	Lamiales	Magnoliopsida	Magnoliophyta
Cypripedium calceolus	Orchidaceae	Asparagales	Liliopsida	Magnoliophyta
Cypripedium fasciculatum	Orchidaceae	Asparagales	Liliopsida	Magnoliophyta
Dactylorhiza lapponica	Orchidaceae	Asparagales	Liliopsida	Magnoliophyta
Danthonia sericea	Poaceae	Poales	Liliopsida	Magnoliophyta
Daucus carota	Apiaceae	Apiales	Magnoliopsida	Magnoliophyta
Dicerandra frutescens	Lamiaceae	Lamiales	Magnoliopsida	Magnoliophyta
Digitalis purpurea	Plantaginaceae	Lamiales	Magnoliopsida	Magnoliophyta
Disporum sessile	Colchicaceae	Liliales	Liliopsida	Magnoliophyta
Echinacea angustifolia	Compositae	Asterales	Magnoliopsida	Magnoliophyta
Eryngium alpinum	Apiaceae	Apiales	Magnoliopsida	Magnoliophyta
Eryngium cuneifolium	Apiaceae	Apiales	Magnoliopsida	Magnoliophyta
Erythronium japonicum	Liliaceae	Liliales	Liliopsida	Magnoliophyta
Eupatorium perfoliatum	Compositae	Asterales	Magnoliopsida	Magnoliophyta
Eupatorium resinosum	Compositae	Asterales	Magnoliopsida	Magnoliophyta
Gentiana pneumonanthe	Gentianaceae	Gentianales	Magnoliopsida	Magnoliophyta
Geum reptans	Rosaceae	Rosales	Magnoliopsida	Magnoliophyta
Geum rivale	Rosaceae	Rosales	Magnoliopsida	Magnoliophyta
Pyrrocoma radiata	Compositae	Asterales	Magnoliopsida	Magnoliophyta
Heliconia acuminata	Heliconiaceae	Zingiberales	Liliopsida	Magnoliophyta
Himantoglossum hircinum	Orchidaceae	Asparagales	Liliopsida	Magnoliophyta
Potentilla congesta	Rosaceae	Rosales	Magnoliopsida	Magnoliophyta
Hyparrhenia diplandra	Poaceae	Poales	Liliopsida	Magnoliophyta
Hypericum cumulicola	Hypericaceae	Theales	Magnoliopsida	Magnoliophyta
Ipomopsis aggregata tenuituba	Polemoniaceae	Solanales	Magnoliopsida	Magnoliophyta
Lepanthes eltoroensis	Orchidaceae	Asparagales	Liliopsida	Magnoliophyta
Lepanthes rubripetala	Orchidaceae	Asparagales	Liliopsida	Magnoliophyta
Lepanthes rupestris	Orchidaceae	Asparagales	Liliopsida	Magnoliophyta
Lepidium davisii	Brassicaceae	Brassicales	Magnoliopsida	Magnoliophyta
Liatris scariosa	Compositae	Asterales	Magnoliopsida	Magnoliophyta
Limonium carolinianum	Plumbaginaceae	Caryophyllales	Magnoliopsida	Magnoliophyta
Linum catharticum	Linaceae	Malpighiales	Magnoliopsida	Magnoliophyta
Lobularia maritima	Brassicaceae	Brassicales	Magnoliopsida	Magnoliophyta
Lomatium bradshawii	Apiaceae	Apiales	Magnoliopsida	Magnoliophyta
Lomatium cookii	Apiaceae	Apiales	Magnoliopsida	Magnoliophyta
Lupinus tidestromii	Leguminosae	Fabales	Magnoliopsida	Magnoliophyta
Minuartia obtusiloba	Caryophyllaceae	Caryophyllales	Magnoliopsida	Magnoliophyta
Nardostachys jatamansi	Caprifoliaceae	Dipsacales	Magnoliopsida	Magnoliophyta
Neotinea ustulata	Orchidaceae	Asparagales	Liliopsida	Magnoliophyta
Anogra deltoidea	Onagraceae	Myrtales	Magnoliopsida	Magnoliophyta
Ophrys sphegodes	Orchidaceae	Asparagales	Liliopsida	Magnoliophyta
Orchis purpurea	Orchidaceae	Asparagales	Liliopsida	Magnoliophyta

<i>Oxalis acetosella</i>	Oxalidaceae	Oxalidales	Magnoliopsida	Magnoliophyta
<i>Paronychia pulvinata</i>	Caryophyllaceae	Caryophyllales	Magnoliopsida	Magnoliophyta
<i>Pinguicula villosa</i>	Lentibulariaceae	Lamiales	Magnoliopsida	Magnoliophyta
<i>Pinguicula vulgaris</i>	Lentibulariaceae	Lamiales	Magnoliopsida	Magnoliophyta
<i>Poa alpina</i>	Poaceae	Poales	Liliopsida	Magnoliophyta
<i>Potentilla anserina</i>	Rosaceae	Rosales	Magnoliopsida	Magnoliophyta
<i>Primula elatior</i>	Primulaceae	Ericales	Magnoliopsida	Magnoliophyta
<i>Primula veris</i>	Primulaceae	Ericales	Magnoliopsida	Magnoliophyta
<i>Primula vulgaris</i>	Primulaceae	Ericales	Magnoliopsida	Magnoliophyta
<i>Pyrrocoma radiata</i>	Compositae	Ericales	Magnoliopsida	Magnoliophyta
<i>Ramonda myconi</i>	Gesneriaceae	Lamiales	Magnoliopsida	Magnoliophyta
<i>Ranunculus acris</i>	Ranunculaceae	Ranunculales	Magnoliopsida	Magnoliophyta
<i>Ranunculus peltatus</i>	Ranunculaceae	Ranunculales	Magnoliopsida	Magnoliophyta
<i>Rubus rigidus</i>	Rosaceae	Rosales	Magnoliopsida	Magnoliophyta
<i>Rubus vitifolius ursinus</i>	Rosaceae	Rosales	Magnoliopsida	Magnoliophyta
<i>Saponaria bellidifolia</i>	Caryophyllaceae	Caryophyllales	Magnoliopsida	Magnoliophyta
<i>Sarcocapnos baetica</i>	Papaveraceae	Ranunculales	Magnoliopsida	Magnoliophyta
<i>Sarcocapnos pulcherrima</i>	Papaveraceae	Ranunculales	Magnoliopsida	Magnoliophyta
<i>Sarracenia purpurea</i>	Sarraceniaceae	Ericales	Magnoliopsida	Magnoliophyta
<i>Saussurea medusa</i>	Compositae	Asterales	Magnoliopsida	Magnoliophyta
<i>Saxifraga aizoides</i>	Saxifragaceae	Saxifragales	Magnoliopsida	Magnoliophyta
<i>Saxifraga cotyledon</i>	Saxifragaceae	Saxifragales	Magnoliopsida	Magnoliophyta
<i>Scabiosa columbaria</i>	Caprifoliaceae	Dipsacales	Magnoliopsida	Magnoliophyta
<i>Setaria incrassata</i>	Poaceae	Poales	Liliopsida	Magnoliophyta
<i>Silene spaldingii</i>	Caryophyllaceae	Caryophyllales	Magnoliopsida	Magnoliophyta
<i>Sporobolus heterolepis</i>	Poaceae	Poales	Liliopsida	Magnoliophyta
<i>Succisa pratensis</i>	Caprifoliaceae	Dipsacales	Magnoliopsida	Magnoliophyta
<i>Themedra triandra</i>	Poaceae	Poales	Liliopsida	Magnoliophyta
<i>Tragopogon pratensis</i>	Compositae	Asterales	Magnoliopsida	Magnoliophyta
<i>Trillium smallii</i>	Melanthiaceae	Liliales	Liliopsida	Magnoliophyta
<i>Trillium camschatcense</i>	Melanthiaceae	Liliales	Liliopsida	Magnoliophyta
<i>Trillium grandiflorum</i>	Melanthiaceae	Liliales	Liliopsida	Magnoliophyta
<i>Trollius laxus</i>	Ranunculaceae	Ranunculales	Magnoliopsida	Magnoliophyta
<i>Viola sagittata ovata</i>	Violaceae	Malpighiales	Magnoliopsida	Magnoliophyta
<i>Zea diploperennis</i>	Poaceae	Poales	Liliopsida	Magnoliophyta
<i>Astrocaryum mexicanum</i>	Arecaceae	Arecales	Liliopsida	Magnoliophyta
<i>Borassus aethiopum</i>	Arecaceae	Arecales	Liliopsida	Magnoliophyta
<i>Calamus rhabdocladus</i>	Arecaceae	Arecales	Liliopsida	Magnoliophyta
<i>Ceratozamia norstogii</i>	Zamiaceae	Cycadales	Cycadophyta	Cycadopsida
<i>Chamaedorea elegans</i>	Arecaceae	Arecales	Liliopsida	Magnoliophyta
<i>Chamaedorea radicalis</i>	Arecaceae	Arecales	Liliopsida	Magnoliophyta
<i>Dioon merolae</i>	Zamiaceae	Cycadales	Cycadophyta	Cycadopsida
<i>Encephalartos cycadifolius</i>	Zamiaceae	Cycadales	Cycadophyta	Cycadopsida
<i>Euterpe edulis</i>	Arecaceae	Arecales	Liliopsida	Magnoliophyta
<i>Euterpe oleracea</i>	Arecaceae	Arecales	Liliopsida	Magnoliophyta
<i>Euterpe precatoria</i>	Arecaceae	Arecales	Liliopsida	Magnoliophyta
<i>Geonoma brevispatha</i>	Arecaceae	Arecales	Liliopsida	Magnoliophyta
<i>Geonoma diversata</i>	Arecaceae	Arecales	Liliopsida	Magnoliophyta
<i>Dypsis decaryi</i>	Arecaceae	Arecales	Liliopsida	Magnoliophyta
<i>Pseudophoenix sargentii</i>	Arecaceae	Arecales	Liliopsida	Magnoliophyta
<i>Rhopalostylis sapida</i>	Arecaceae	Arecales	Liliopsida	Magnoliophyta
<i>Sabal yapa</i>	Arecaceae	Arecales	Liliopsida	Magnoliophyta
<i>Adesmia volckmannii</i>	Leguminosae	Fabales	Magnoliopsida	Magnoliophyta
<i>Ambrosia deltoidea</i>	Compositae	Asterales	Magnoliopsida	Magnoliophyta
<i>Ambrosia dumosa</i>	Compositae	Asterales	Magnoliopsida	Magnoliophyta
<i>Dubautia sandwicensis</i>	Compositae	Asterales	Magnoliopsida	Magnoliophyta
<i>Atriplex acanthocarpa</i>	Amaranthaceae	Caryophyllales	Magnoliopsida	Magnoliophyta
<i>Atriplex canescens</i>	Amaranthaceae	Caryophyllales	Magnoliopsida	Magnoliophyta
<i>Atriplex vesicaria</i>	Amaranthaceae	Caryophyllales	Magnoliopsida	Magnoliophyta
<i>Banksia ericifolia</i>	Proteaceae	Proteales	Magnoliopsida	Magnoliophyta
<i>Calluna vulgaris</i>	Ericaceae	Ericales	Magnoliopsida	Magnoliophyta
<i>Cassia nemophila</i>	Leguminosae	Fabales	Magnoliopsida	Magnoliophyta

Eremophila maitlandii	Scrophulariaceae	Lamiales	Magnoliopsida	Magnoliophyta
Gardenia actinocarpa	Rubiaceae	Gentianales	Magnoliopsida	Magnoliophyta
Helianthemum juliae	Cistaceae	Malvales	Magnoliopsida	Magnoliophyta
Lindera umbellata	Lauraceae	Laurales	Magnoliopsida	Magnoliophyta
Magnolia salicifolia	Magnoliaceae	Magnoliales	Magnoliopsida	Magnoliophyta
Miconia albicans	Melastomataceae	Myrtales	Magnoliopsida	Magnoliophyta
Mulinum spinosum	Apiaceae	Apiales	Magnoliopsida	Magnoliophyta
Petrophile pulchella	Proteaceae	Proteales	Magnoliopsida	Magnoliophyta
Purshia subintegra	Rosaceae	Rosales	Magnoliopsida	Magnoliophyta
Schmaltzia copallinum	Anacardiaceae	Sapindales	Magnoliopsida	Magnoliophyta
Senecio filaginoides	Compositae	Asterales	Magnoliopsida	Magnoliophyta
Viburnum furcatum	Adoxaceae	Dipsacales	Magnoliopsida	Magnoliophyta
Echeveria longissima	Crassulaceae	Saxifragales	Magnoliopsida	Magnoliophyta
Echinocactus platyacanthus	Cactaceae	Caryophyllales	Magnoliopsida	Magnoliophyta
Coespeletia spicata	Compositae	Asterales	Magnoliopsida	Magnoliophyta
Coespeletia timotensis	Compositae	Asterales	Magnoliopsida	Magnoliophyta
Mammillaria crucigera	Cactaceae	Caryophyllales	Magnoliopsida	Magnoliophyta
Mammillaria gaumeri	Cactaceae	Caryophyllales	Magnoliopsida	Magnoliophyta
Mammillaria huitzilopochtli	Cactaceae	Caryophyllales	Magnoliopsida	Magnoliophyta
Neobuxbaumia macrocephala	Cactaceae	Caryophyllales	Magnoliopsida	Magnoliophyta
Neobuxbaumia mezcalaensis	Cactaceae	Caryophyllales	Magnoliopsida	Magnoliophyta
Neobuxbaumia tetetzo	Cactaceae	Caryophyllales	Magnoliopsida	Magnoliophyta
Opuntia macrocentra	Cactaceae	Caryophyllales	Magnoliopsida	Magnoliophyta
Pterocereus gaumeri	Cactaceae	Caryophyllales	Magnoliopsida	Magnoliophyta
Abies concolor	Pinaceae	Pinales	Pinopsida	Pinophyta
Abies magnifica	Pinaceae	Pinales	Pinopsida	Pinophyta
Acer palmatum	Sapindaceae	Sapindales	Magnoliopsida	Magnoliophyta
Acer mono	Sapindaceae	Sapindales	Magnoliopsida	Magnoliophyta
Acer rufinerve	Sapindaceae	Sapindales	Magnoliopsida	Magnoliophyta
Acer saccharum	Sapindaceae	Sapindales	Magnoliopsida	Magnoliophyta
Aquilaria crassna	Thymelaeaceae	Malvales	Magnoliopsida	Magnoliophyta
Araucaria hunsteinii	Araucariaceae	Pinales	Pinopsida	Pinophyta
Araucaria laubenfelsii	Araucariaceae	Pinales	Pinopsida	Pinophyta
Avicennia germinans	Acanthaceae	Lamiales	Magnoliopsida	Magnoliophyta
Bertholletia excelsa	Lecythidaceae	Ericales	Magnoliopsida	Magnoliophyta
Calocedrus decurrens	Cupressaceae	Pinales	Pinopsida	Pinophyta
Chlorocardium rodiei	Lauraceae	Laurales	Magnoliopsida	Magnoliophyta
Dacrydium elatum	Podocarpaceae	Pinales	Pinopsida	Pinophyta
Dicymbe altsonii	Leguminosae	Fabales	Magnoliopsida	Magnoliophyta
Duguetia neglecta	Annonaceae	Magnoliales	Magnoliopsida	Magnoliophyta
Entandrophragma cylindricum	Meliaceae	Sapindales	Magnoliopsida	Magnoliophyta
Fagus grandifolia	Fagaceae	Fagales	Magnoliopsida	Magnoliophyta
Khaya senegalensis	Meliaceae	Sapindales	Magnoliopsida	Magnoliophyta
Magnolia macrophylla dealbata	Magnoliaceae	Magnoliales	Magnoliopsida	Magnoliophyta
Manilkara zapota	Sapotaceae	Ericales	Magnoliopsida	Magnoliophyta
Pentaclethra macroloba	Leguminosae	Fabales	Magnoliopsida	Magnoliophyta
Phyllanthus emblica	Phyllanthaceae	Malpighiales	Magnoliopsida	Magnoliophyta
Phyllanthus indofischeri	Phyllanthaceae	Malpighiales	Magnoliopsida	Magnoliophyta
Pinus lambertiana	Pinaceae	Pinales	Pinopsida	Pinophyta
Pinus nigra	Pinaceae	Pinales	Pinopsida	Pinophyta
Pinus palustris	Pinaceae	Pinales	Pinopsida	Pinophyta
Pinus sylvestris	Pinaceae	Pinales	Pinopsida	Pinophyta
Platymiscium filipes	Leguminosae	Fabales	Magnoliopsida	Magnoliophyta
Prioria copaifera	Leguminosae	Fabales	Magnoliopsida	Magnoliophyta
Prosopis glandulosa	Leguminosae	Fabales	Magnoliopsida	Magnoliophyta
Prosopis laevigata	Leguminosae	Fabales	Magnoliopsida	Magnoliophyta
Prunus africana	Rosaceae	Rosales	Magnoliopsida	Magnoliophyta
Prunus serotina	Rosaceae	Rosales	Magnoliopsida	Magnoliophyta
Quercus mongolica crispula	Fagaceae	Fagales	Magnoliopsida	Magnoliophyta
Quercus rugosa	Fagaceae	Fagales	Magnoliopsida	Magnoliophyta
Rhizophora mangle	Rhizophoraceae	Malpighiales	Magnoliopsida	Magnoliophyta
Rhododendron ponticum	Ericaceae	Ericales	Magnoliopsida	Magnoliophyta

Triadica sebifera	Euphorbiaceae	Malpighiales	Magnoliopsida	Magnoliophyta
Scaphium macropodum	Malvaceae	Malvales	Magnoliopsida	Magnoliophyta
Stryphnodendron microstachyum	Leguminosae	Fabales	Magnoliopsida	Magnoliophyta
Swietenia macrophylla	Meliaceae	Sapindales	Magnoliopsida	Magnoliophyta
Tachigali vasquezii	Leguminosae	Fabales	Magnoliopsida	Magnoliophyta
Tsuga canadensis	Pinaceae	Pinales	Pinopsida	Pinophyta

Appendix 3: Elasticity and climatic Principal Component Analysis

Here we provide the loadings and variance explained by each axis in the Principal Component Analysis (PCA) describing the elasticities of the 550 transition matrices used in our analysis (Table S2).

Table S2. Rotations and variance explained for each axis of the Principle Component Analysis performed on matrix element elasticities, z_n

Rotation on	Axis			
	PC1	PC2	PC3	PC4
$\delta_{progr,n}$	-0.561	0.082	0.676	0.470
$\delta_{retro,n}$	-0.177	0.878	-0.396	0.204
$\delta_{stasis,n}$	0.650	-0.038	0.015	0.759
$\delta_{repro,n}$	-0.482	-0.471	-0.621	0.401
Importance of components				
Standard deviation	1.540	1.047	0.730	0.009
Proportion variance	0.593	0.274	0.133	0.00002
Cumulative proportion	0.593	0.867	1	1

We used eight BioClim temperature variables to describe the climate of each location (shown in Appendix 4, Table S4) which were highly correlated with each other. We summarise eight BioClim temperature variables (Table S3) using a PCA, carried out with the `prcomp` function in R (R Core Team, 2013). All variables were centred on 0 and scaled to have unit variance so that the units a variable was reported in did not influence the results. This PCA revealed that mean annual temperature is positively correlated with all the other temperature variables except seasonality (`bio_4`), and temperature range (`bio_7`), with which it is negatively correlated (Figure S1c). The first PC axis, which we refer to as `PC_temp`, explains 71% of the variance in temperature variables. `PC_temp` represents a gradient from cooler seasonably variable temperate climates to hot, non-seasonal tropical climates (Figure S1a). See Table S3 for loadings and variance explained by each axis. We use aridity index (AI) and precipitation seasonality to describe precipitation at each location. AI is positively correlated to some degree with all the other precipitation variables in BioClim (Appendix 4, Table S4), except for precipitation seasonality (`bio_15`), with which it has

little correlation (Figure S1d). We took the natural log of AI because small differences in water availability have large ecological and biological effects in very arid areas, while that same small difference in water availability would have almost no affect in a high precipitation region.

Table S3. Rotations and variance explained for each axis of the Principle Component Analysis performed on the temperature BioClim variables. See Table S4, Appendix 4 for a definition of each BioClim variable.

Rotation on	Axis							
	PC1	PC2	PC3	PC4	PC5	PC6	PC7	PC 8
bio_1	0.405	-0.207	0.020	-0.148	0.226	-0.089	0.844	0.000
bio_3	0.380	0.088	-0.086	0.831	-0.078	-0.378	-0.032	0.000
bio_4	-0.373	-0.371	-0.039	-0.179	-0.098	-0.825	-0.003	0.000
bio_5	0.270	-0.619	-0.267	-0.005	0.399	0.124	-0.370	0.402
bio_6	0.414	0.069	0.039	-0.266	0.315	-0.199	-0.334	-0.708
bio_7	-0.318	-0.513	-0.233	0.321	-0.108	0.328	0.152	-0.581
bio_8	0.273	-0.402	0.733	-0.017	-0.454	0.080	-0.120	-0.000
bio_9	0.365	-0.008	-0.571	-0.286	-0.676	0.008	-0.032	-0.000
Importance of components								
Standard deviation	2.379	1.181	0.799	0.493	0.206	0.123	0.077	0.000
Proportion of variance	0.708	0.174	0.080	0.030	0.005	0.002	0.001	0.000
Cumulative Proportion	0.708	0.882	0.962	0.992	0.997	0.999	1.000	1.000

We map the location of each population in geographic and environmental space, defined by two important environmental variables in the temperature PCA, mean temperature and seasonality (bio_1 and bio_4, Figure S1b and c). There are multiple, geographically spread populations in both temperate and tropical regions (Figure S1a).

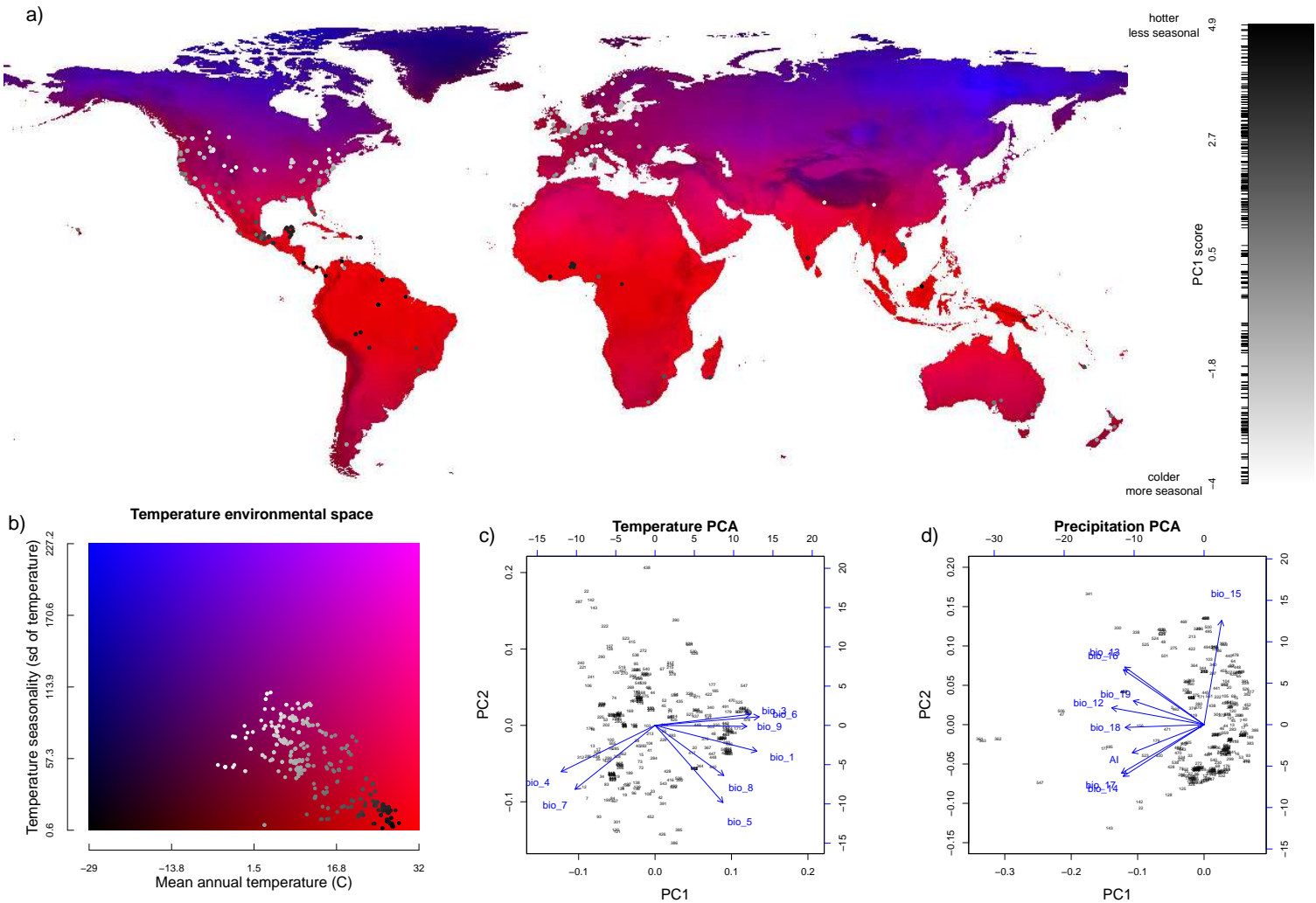


Figure S1. Study locations in geographic and temperature space. Full caption on next page.

Figure S1. Study locations in geographic and temperature space for the 550 transition matrices, pertaining to 210 species, used to test how generalisable demographic performance is between species and locations. a) World map with a two channel colour palette, with red representing mean annual temperature and blue representing seasonal variability in temperature (environmental space shown in b). Red areas are characterised by high temperatures year-round (tropics), whereas blue areas by lower mean temperatures, but large seasonal fluctuations in temperature (high latitude continental). Purple represents regions with both high temperatures and high seasonality while dark regions have low temperatures year-round. Points show the geographic location of the studies used (a) and their position in the 2 dimensional temperature space (b). In a) and b) colour of the points show their Principal Component score on the first axis (PC1) based on a principal component analysis using BioClim temperature variables. PC1 explained 71% of variation in the data. Ticks on the PC1 legend in a) show the score of each transition matrix on PC1 axis. c) shows the intensity (arrow length) and loading (angle onto each PC) for the temperature PCA (Table S5, Appendix 4). d) shows intensity (arrow length) and loading (angle onto each PC) for the precipitation PCA (see variables in Table S4, Appendix 4).

Appendix 4: Predictor variables

The three environmental predictor variables used in our statistical analysis were chosen or derived from the environmental variables in Table S4.

Table S4. Raw environmental covariates. All temperature and precipitation values were extracted from BioClim (<http://worldclim.org/current>) for each GPS-location reported in the COMPADRE Plant Matrix Database. Values for AI were taken from CGIAR-CSI GeoPortal (<http://www.csi.cgiar.org>). All values were averaged over the surrounding 2km to help buffer uncertainty in the reported locations. Source label indicates the name of the covariate in the respective data source.

source label	Units	Description
<i>Temperature</i>		
bio_1	C ⁰ × 10	annual mean temperature
bio_3	ratio	Isothermality = $\frac{\text{mean diurnal range}}{\text{annual range}} \times 100$
bio_4	stdev × 100	temperature seasonality
bio_5	C ⁰ × 10	max temperature of warmest month
bio_6	C ⁰ × 10	min temperature of coldest month
bio_7	C ⁰ × 10	temperature annual range (bio_5 - bio_6)
bio_8	C ⁰ × 10	mean temperature of wettest quarter
bio_9	C ⁰ × 10	mean temperature of driest quarter
<i>Precipitation</i>		
AI	ratio	Aridity index = $\frac{\text{mean annual precipitation}}{\text{Mean Annual Potential Evapo-Transpiration}}$
bio_12	mm	annual precipitation
bio_13	mm	precipitation of wettest month
bio_14	mm	precipitation of driest month
bio_15	coef var	precipitation seasonality
bio_16	mm	precipitation of wettest quarter
bio_17	mm	precipitation of driest quarter
bio_18	mm	precipitation of warmest quarter
bio_19	mm	precipitation of coldest quarter

Temperature variables were reduced to one axis with a Principal Component Analysis (PCA) (see Table S2, Appendix 3 for rotations and importance of each PCA axis). A PCA on the precipitation variables showed that they were all positively correlated with each other, except precipitation seasonality, which was not correlated with the other variables. We therefore used aridity

index and precipitation seasonality to represent precipitation in the models. These three environmental predictors, along with three non-environmental predictors, spatial location and phylogenetic relationships are used to predict all four demographic metrics, $\ln(\lambda)$, $\ln(\text{CV}(\lambda) + 1)$, $\ln(\rho)$ and SPG. These predictors are briefly outlined in Table S5.

Table S5. Non-environmental and environmental covariates. See Table S4 for details of environmental covariate sources and extraction. Source label gives the name of the covariate in the respective data source.

Predictor	Units	Description	source
<i>Non-environmental predictors</i>			
geo_loc	degrees	latitude and longitude of study site	CPMD [▲]
phylogeny		position of each species in a phylogenetic tree	Salguero-Gómez <i>et al.</i> (2015)
dimension		number of rows in matrix	CPMD
life_expect	years	average life expectancy in the sample populations	calculated from matrices in CPMD
growth_form	binary factor	indicates if species is a herbaceous perennial	CPMD
<i>Environmental predictors</i>			
PC_temp	unitless scale	principle component score on the first axis that combines 8 correlated temperature variables. The PC scores reflect a gradient from tropical (warm stable temperatures), to temperate locations (cooler, seasonally variable temperatures)	worldclim.org/bioclim [■]
Aridity index		measure of water stress that includes precipitation and temperature	CGIAR-CSI [♦]
precip_seasonality	CV	coefficient of variation in precipitation over a year	worldclim.org/bioclim
[▲] Date from COMPADRE Plant Matrix Database retrieved from www.compadre-db.org/ on 4/12/2013 [■] Date from worldclim.org/bioclim retrieved from http://worldclim.org/current , using ESIR 30 arc-seconds grids on 27/2/2014 [♦] Consortium for Spatial Information CGIAR-CSI, from http://www.csi.cgiar.org on 27/2/2014			

Appendix 5: Phylogenetic and spatial decay curves for all models and demographic metrics

Figures S2 - S5 show the decay curves for each demographic metric, for each model structure we tested. Negative exponential decay models underpin the spatial and phylogenetic prediction terms. The way predictive support decreases with distance suggests the spatial and phylogenetic scale at which demographic processes are influenced. Colour indicates the model structure. The 'main_int' model includes all predictors and two-way interactions, along with spatial and phylogenetic predictor terms, with predictions based on all populations. The 'main' model includes only the six main effects, along with geographic and phylogenetic predictor terms, with predictions based on all populations. Models denoted 'phygeo' only includes the spatial and phylogenetic predictor terms, models denoted 'geo' only include the spatial predictor term, and models denoted 'phy' only include the phylogenetic predictor term. The spatial and phylogenetic prediction terms of models denoted 'allpops' have predictions based on all populations. Those denoted 'noself' have spatial predictions based only on populations that were not in the same location and the phylogenetic predictions based only on populations that were not the same species.

Note that uncertainty around the estimated curve can change dramatically between model structures predicting the same demographic metric. However, the explanatory power of some models is much higher than others (i.e. they have higher R^2). It is also important to remember that these curves represent an average across all species and environments. A curve based on populations in different environments (e.g. mountainous regions), or any single species, might look very different.

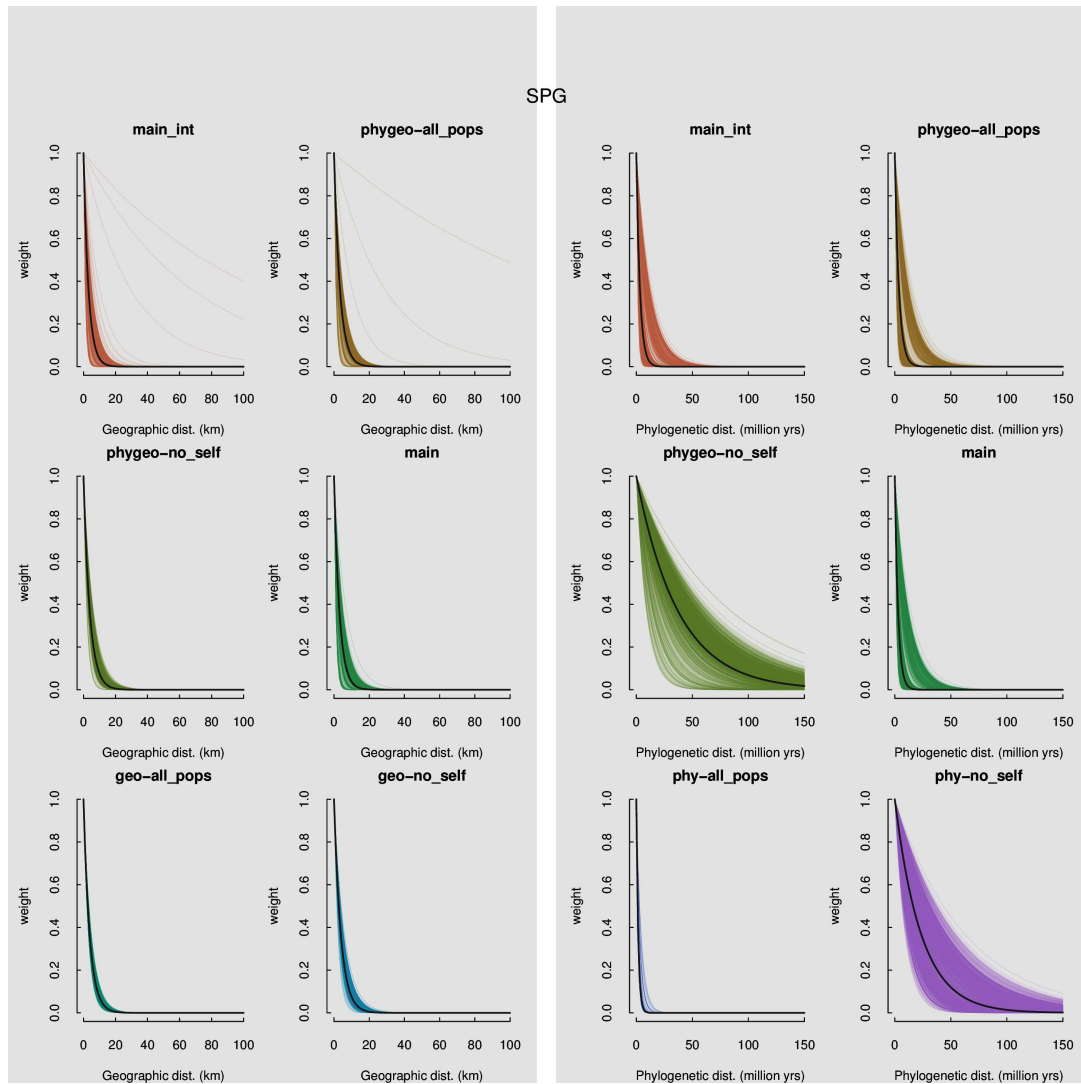


Figure S2. Decay curves of the spatial and phylogenetic predictive terms for each model for SPG. Coloured lines show the curve produced by the estimated decay parameter for each of the 1500 MCMC samples. Grey lines show the average curve, taken over all 1500 MCMC samples.

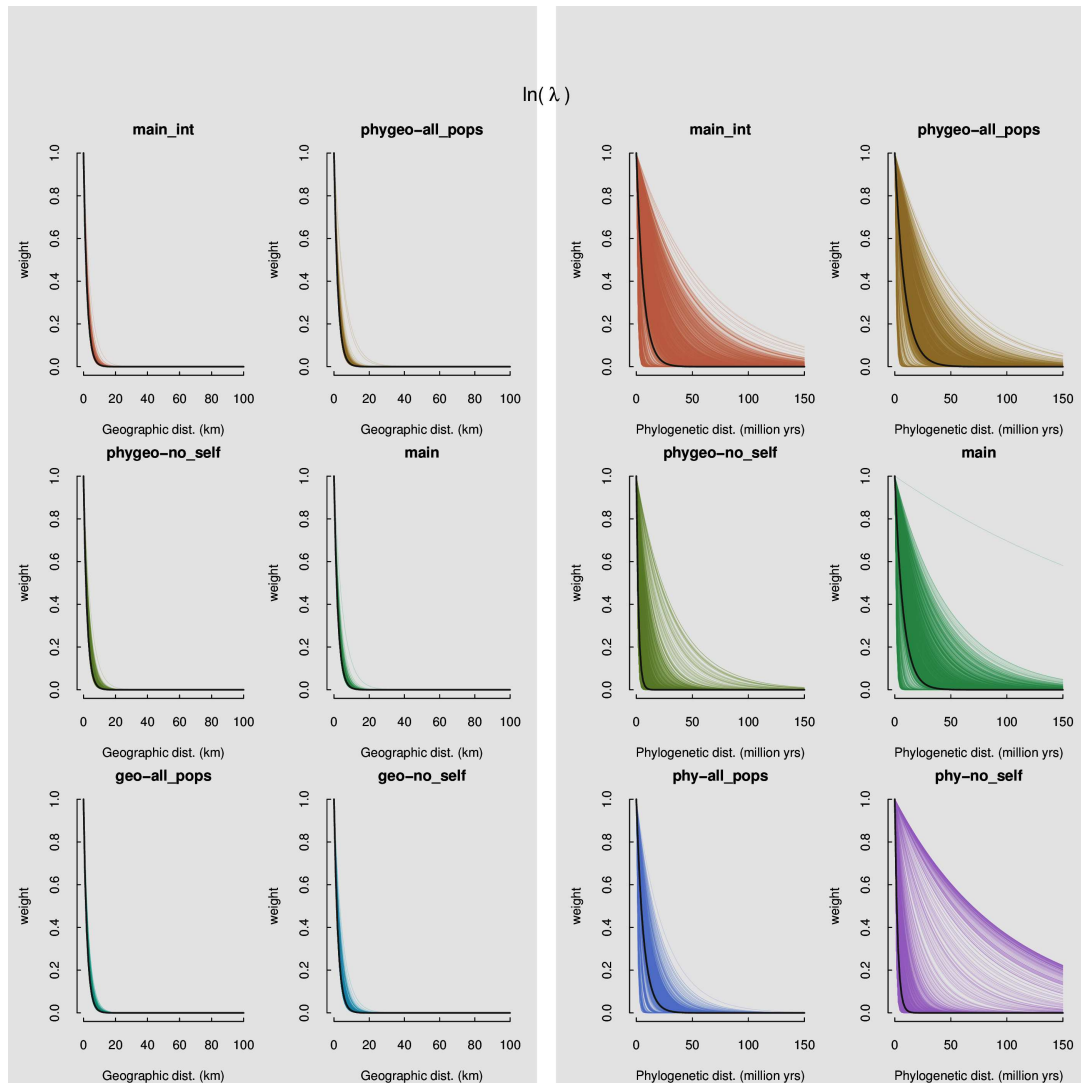


Figure S3. Decay curves of the spatial and phylogenetic predictive terms for each model for $\ln(\lambda)$. Coloured lines show the curve produced by the estimated decay parameter for each of the 1500 MCMC samples. Grey lines show the average curve, taken over all 1500 MCMC samples.

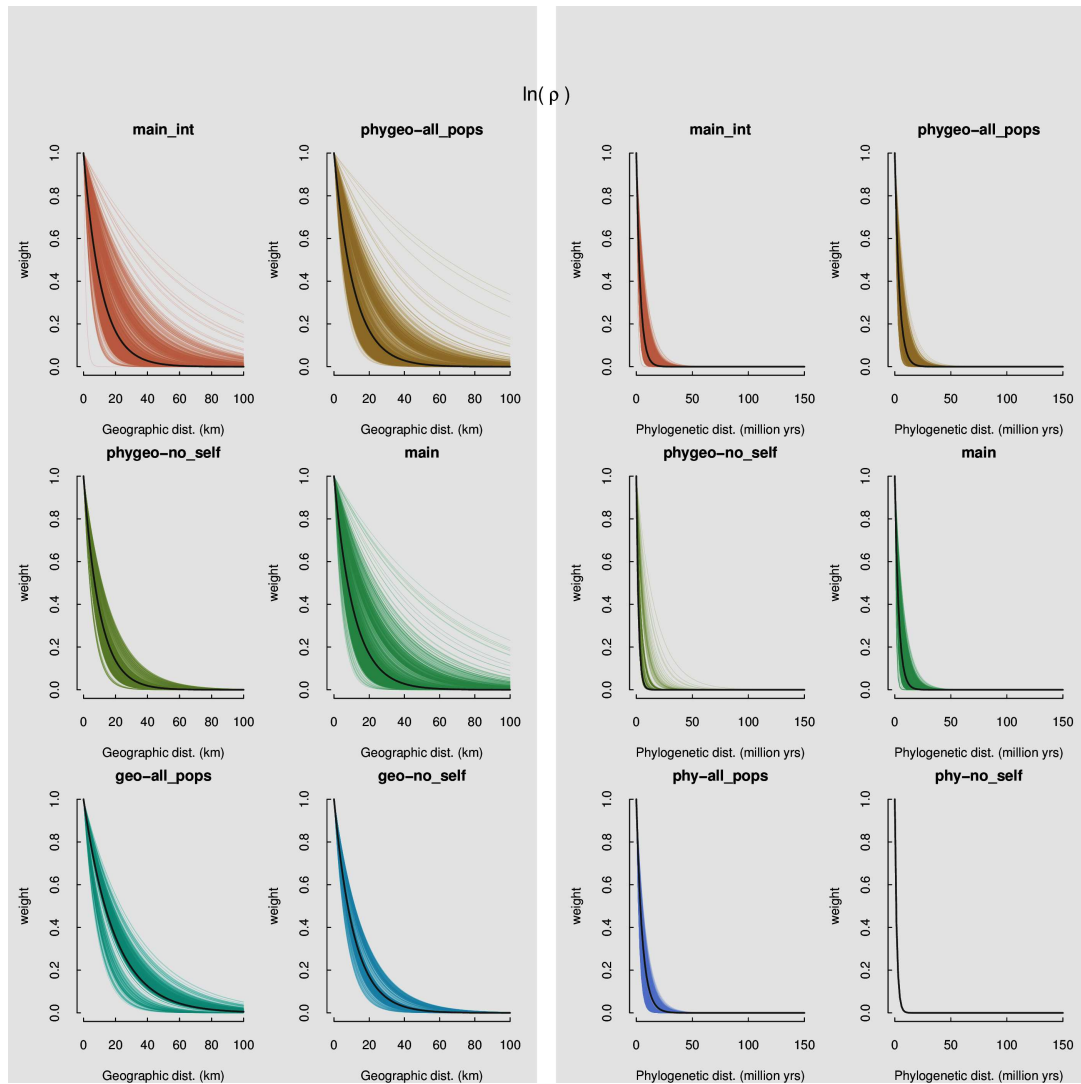


Figure S4. Decay curves of the spatial and phylogenetic predictive terms for each model for $\ln(\rho)$. Coloured lines show the curve produced by the estimated decay parameter for each of the 1500 MCMC samples. Grey lines show the average curve, taken over all 1500 MCMC samples.

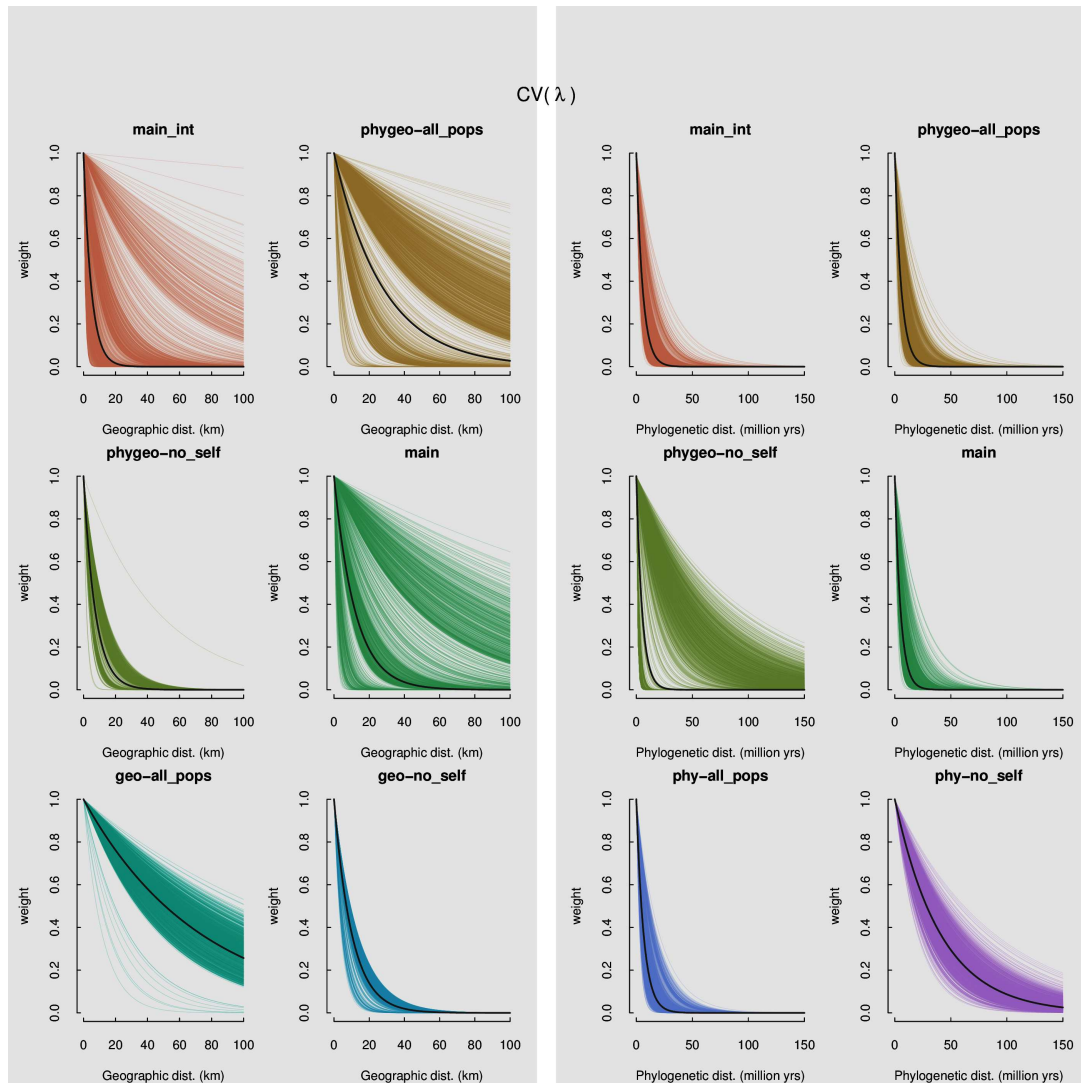


Figure S5. Decay curves of the spatial and phylogenetic predictive terms for each model for $CV(\lambda)$. Coloured lines show the curve produced by the estimated decay parameter for each of the 1500 MCMC samples. Grey lines show the average curve, taken over all 1500 MCMC samples.